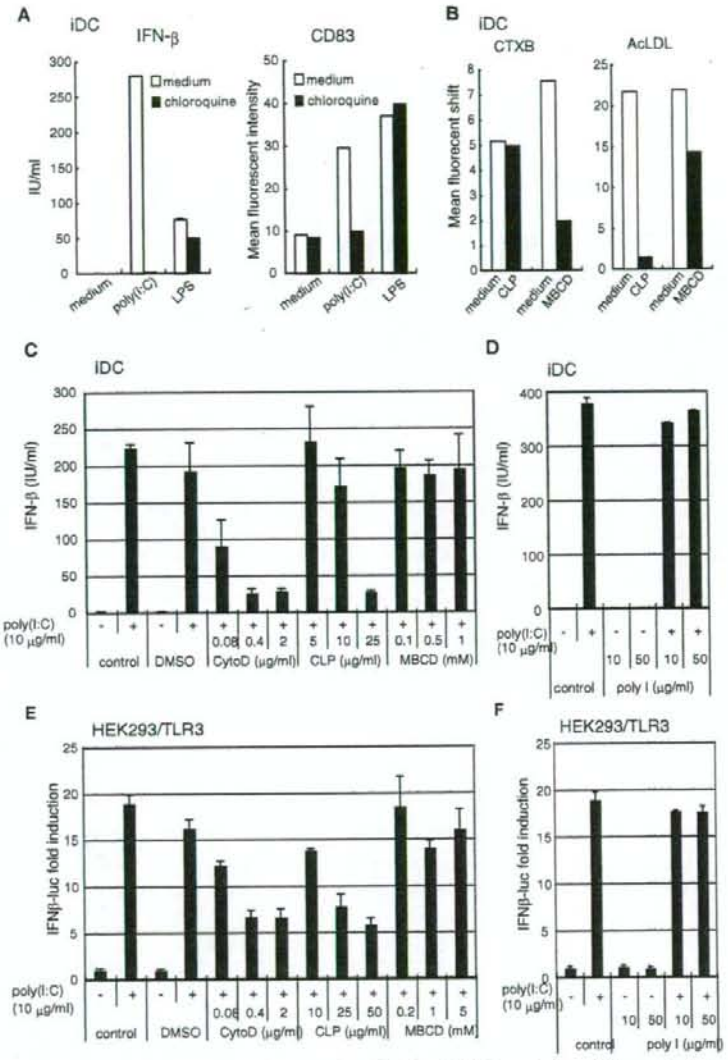

FIGURE 2. A clathrin-dependent endocytic pathway participates in poly(I:C)-induced IFN-β production. *A*, Monocyte-derived iDCs were preincubated with medium alone or 5 μg/ml chloroquine for 2 h and then stimulated with medium alone, 10 μg/ml polymyxin B-treated poly(I:C), or 100 ng/ml LPS. After 24 h, the culture medium was collected, and the amount of IFN-β was determined by an ELISA kit; the cells were then washed, and CD83 up-regulation was assessed by flow cytometry. *B*, Specificity of pharmacological inhibitors for clathrin-dependent and -independent endocytic pathways. iDCs were pretreated with 25 μg/ml chlorpromazine (CLP), 1 mM methyl-β-cyclodextrin (MBCD), or medium alone for 1 h at 37°C and subsequently incubated with 0.2 μM AlexaFluor 488-AcLDL or 5 μg/ml AlexaFluor 488-CTXB for 30 min at 4°C. The cells were then warmed for 5 min at 37°C to allow endocytosis to occur. After quenching the fluorescence of uningested AlexaFluor-488 AcLDL or AlexaFluor-488 CTXB, the cells were analyzed by flow cytometry. The similar results were obtained by using HEK293 cells (data not shown). *C*, Poly(I:C)-induced IFN-β production in monocyte-derived iDCs in the presence of inhibitors of the endocytic pathway. iDCs (1×10^6/ml) were preincubated with the indicated concentrations of cytochalasin D (CytoD), MBCD, or CLP for 1 h and then stimulated with 10 μg/ml poly(I:C). As a buffer control for CytoD, DMSO (final concentration 0.1%) was added to cells. After 24 h, the amount of IFN-β in the culture supernatant was assessed by ELISA kit. The viability of the cells was estimated with propidium iodide staining at the time of supernatant collection. iDCs: CytoD, 0 μg/ml (93.56%), 0.08 μg/ml (93.61%), 0.4 μg/ml (93.25%), 2 μg/ml (66.43%); CLP, 5 μg/ml (91.8%), 10 μg/ml (90.0%), 25 μg/ml (65.3%); MBCD, 0.1 mM (94.7%), 0.5 mM (90.0%), 1 mM (88.0%). HEK293 cells: CytoD, 0 μg/ml (93.57%), 0.08 μg/ml (90.08%), 0.4 μg/ml (81.10%), 2 μg/ml (73.24%); CLP, 10 μg/ml (93.8%), 25 μg/ml (87.0%), 50 μg/ml (86.0%); MBCD 0.2 mM (93.0%), 1 mM (86.5%), 5 mM (71.5%). *D*, iDCs were preincubated with the indicated poly I concentrations for 1 h and then stimulated with 10 μg/ml poly(I:C) for 24 h. *E* and *F*, Poly(I:C)-induced IFN-β promoter activation in TLR3-expressing HEK293 cells in the presence of inhibitors of the endocytic pathway (*E*) or poly I (*F*). HEK293 cells in 24-well plates were transfected with pEFBOS/hTLR3 together with the reporter plasmid. Twenty-four hours after transfection, the cells were washed and pretreated with the indicated concentrations of inhibitors or poly I for 1 h and then stimulated with 10 μg/ml poly(I:C). After 6 h, the luciferase reporter activities were measured and expressed as the fold induction relative to the activity of unstimulated cells. Representative data from a minimum of three separate experiments are shown.

Flow cytometry

Monocyte-derived iDCs were pretreated with medium alone or 5 μg/ml chloroquine for 2 h at 37°C and then stimulated with 100 ng/ml LPS or 10 μg/ml polymyxin B treated-poly(I:C) for 24 h. After washing, cells were incubated with mouse IgG1, or anti-CD83 mAb (1 μg) in the presence of human IgG (10 μg) for 30 min at 4°C in FACS buffer (DPBS containing 0.5% BSA and 0.1% sodium azide). After the cells were washed twice with the above buffer, FITC-labeled secondary Ab (American Qualex) was added and the cells were further incubated for 30 min at 4°C. In the case of dsRNA binding assay, cells were incubated with the indicated concentrations of poly(I:C) or N500 in culture medium for 30 min at 4°C. After washing, cells were labeled with anti-dsRNA mAb (K1) or control mouse IgG2a (1 μg) for 30 min at 4°C and then incubated with FITC-labeled secondary Ab. The cells were analyzed on a FACSCalibur (BD Biosciences). For examination of binding and internalization of ODNs, iDCs were incubated with FITC-labeled ODN2006 or ODN2216 in the presence or absence of poly(I:C) for 2 h at 37°C. After washing, cells were analyzed on FACSCalibur.

Confocal microscopy

Monocyte-derived iDCs (1×10^6/ml) were incubated with 2 μM FITC-ODN2006 for 30 min at 37°C. Cells were washed three times and treated with permeabilizing solution (BD Biosciences) for 10 min at room temperature. After washing, cells were stained with mouse IgG1 or anti-TLR3 mAb (TLR3.7) (20 μg/ml) in FACS buffer for 1 h at room temperature. Alexa Fluor 568-conjugated secondary Ab (1/400 diluted with PBS containing 10% BlocAce and 10% goat serum) was used to visualize staining of the primary Abs. Nuclei were stained with DAPI (2 μg/ml in PBS) for 10 min before mounting onto glass slides using PBS containing 2.3% DABCO and 50% glycerol. Cells were visualized at a magnification of ×63 with an LSM510 META microscope (Zeiss).

Results

Unresponsiveness of mDCs to synthetic virus-derived dsRNA

mDCs express TLR3 intracellularly and produce IFN-β in response to poly(I:C), which is a synthetic TLR3 ligand (10). To analyze the mechanism by which mDCs recognize extracellular dsRNA, we examined whether synthetic virus-derived dsRNA activates DCs to produce IFN-β. dsRNAs of various lengths were in vitro transcribed using MV cDNA encoding N-protein as the template. First, we examined the abilities of synthetic dsRNAs to activate the IFN-β promoter in HEK293 cells transiently expressing human TLR3, which predominantly express TLR3 intracellularly but possess some TLR3 molecules on the cell surface. The TLR3-acitivating abilities of these dsRNAs were remarkably lower than that of poly(I:C) when extracellularly added to the cells (Fig. 1*A*, *left panel*), while they significantly activated TLR3 when introduced into the cells using a cationic liposome DOTAP (Fig. 1*A*, *center* and *right panel*). Next, the DC-activating abilities of these dsRNAs were analyzed by measuring IFN-β production in monocyte-derived iDCs. The synthetic dsRNAs failed to induce IFN-β production in iDCs (Fig. 1*B*, *left panel*), as previously observed (21). In contrast, when dsRNA was targeted to endosomal TLR3 using DOTAP, all MV-N-derived dsRNAs induced IFN-β production at a level that was similar to or higher than that from poly(I:C) stimulation (Fig. 1*B*, *right panel*). Since these in vitro-transcribed dsRNAs contain 5′-ppp, we treated dsRNA with CIAP. Once again, extracellular CIAP-treated dsRNAs did not induce IFN-β production in iDCs, suggesting that the DC-activating ability of dsRNA is independent of its 5′ structure (Fig. *1C*).

The clathrin-mediated endocytic pathway participates in dsRNA-induced IFN-β production

Poly(I:C)-induced IFN-β production and costimulatory molecule (CD83) up-regulation were inhibited by pretreatment of the cells with chloroquine, an inhibitor of endosomal maturation (Fig. 2*A*). The endocytic pathway that participates in TLR3-mediated signaling was analyzed using the pharmacological

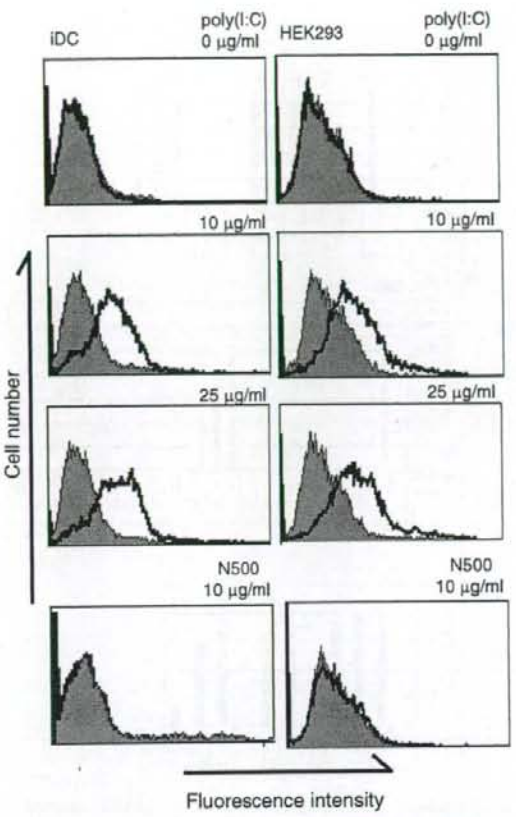

FIGURE 3. Flow cytometric analysis of poly(I:C) binding to DCs and HEK293 cells. Monocyte-derived iDCs and HEK293 cells were incubated with the indicated concentrations of poly(I:C) or N500 in the culture medium for 30 min at 4°C. After washing, the cells were stained with anti-dsRNA mAb (K1) and FITC-labeled secondary Ab (solid line). Shaded histograms represent cells labeled with isotype-matched control Ab.

inhibitors cytochalasin D (a phagocytosis inhibitor), methyl-β-cyclodextrin (a caveolae-mediated endocytosis inhibitor) (23–25), and chlorpromazine (a clathrin-mediated endocytosis inhibitor) (23, 26). We first evaluated various concentrations of these inhibitors to maximize their specificity and eliminate toxic side effects. Under the experimental setting, cell damage was negligible within the concentrations of the inhibitors used in this study. Under optimized conditions, chlorpromazine inhibited the internalization of AlexaFluor 488-AcLDL, a marker for the clathrin-dependent pathway (27), but had no effect on the uptake of AlexaFluor 488-CTXB, a marker for caveolar-mediated internalization (28). In contrast, methyl-β-cyclodextrin significantly inhibited the internalization of AlexaFluor 488-CTXB, but had few effects on AlexaFluor 488-AcLDL uptake (Fig. 2*B*). IFN-β production was inhibited by pretreatment of iDCs with cytochalasin D and chlorpromazine but not with methyl-β-cyclodextrin, suggesting that the clathrin-dependent endocytic pathway mediates cell entry of poly(I:C) to induce IFN-β gene transcription (Fig. 2*C*). In addition, poly I, an inhibitor of scavenger receptors (29), did not block poly(I:C)-induced IFN-β production in iDCs (Fig. 2*D*). Although poly I has been shown to activate TLR3 in murine B cells and bone

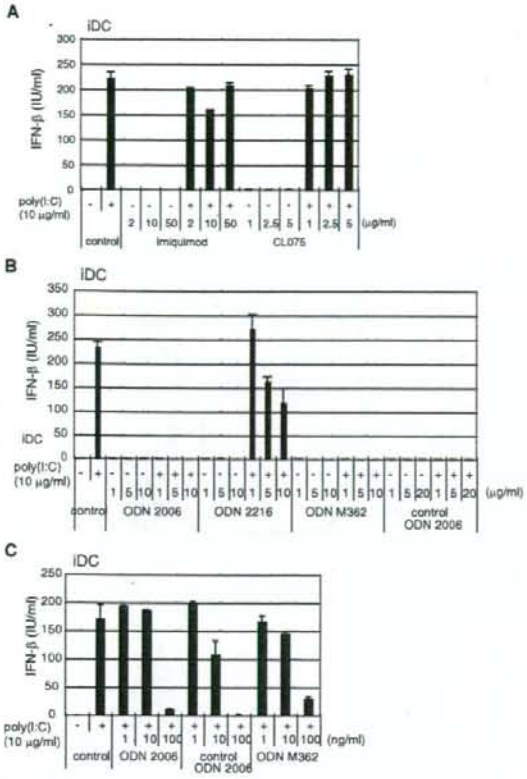

FIGURE 4. B- and C-type ODNs inhibit poly(I:C)-induced IFN-β production in DCs. Monocyte-derived iDCs (1×10^6/ml) were preincubated with the indicated concentrations of Imiquimod (TLR7 ligand), CL075 (TLR8 ligand) (*A*), ODN2006 (B-type TLR9 ligand), ODN2216 (A-type TLR9 ligand), ODNM362 (C-type TLR9 ligand), or control ODN2006 (*B* and *C*) for 1 h and then stimulated with 10 μg/ml poly(I:C). After 24 h, the amount of IFN-β in the culture supernatant was assessed by ELISA.

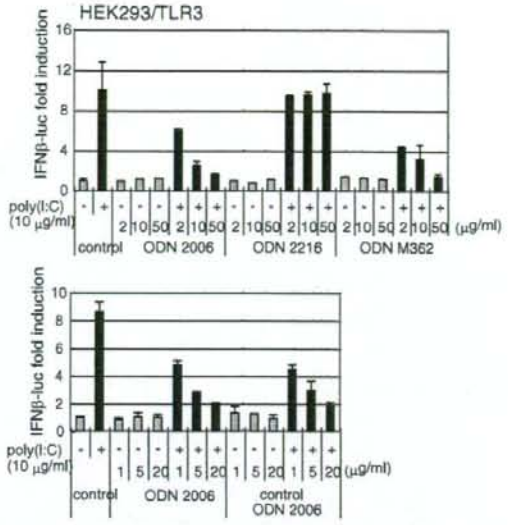

FIGURE 5. B- and C-type ODNs inhibit poly(I:C)-induced TLR3-mediated IFN-β promoter activation. HEK293 cells in 24-well plates were transfected with pEFBOS/hTLR3 together with the reporter plasmid. Twenty-four hours after transfection, the cells were washed and preincubated with the indicated concentrations of ODN2006, ODN2216, or ODNM362 for 1 h and then stimulated with 10 μg/ml poly(I:C). After 6 h, the luciferase reporter activities were measured and expressed as the fold induction relative to the activity of unstimulated cells. Representative data from a minimum of three separate experiments are shown.

marrow-derived DCs (30), human monocyte-derived iDCs could not produce IFN-β in response to extracellular poly I. Similar results were obtained with TLR3-expressing HEK293 cells (Fig. 2, *E* and *F*). Poly(I:C)-induced TLR3-mediated IFN-β promoter activation was inhibited by pretreatment of cells with cytochalasin D and chlorpromazine but not with methyl-β-cyclodextrin or poly I.

Poly(I:C) binding to mDCs

The potent IFN-β-inducing ability of poly(I:C) may be due to the uptake of the latter by iDCs. To test poly(I:C) binding to unknown cell-surface receptors, iDCs and HEK293 cells were incubated with various poly(I:C) concentrations at 4°C for 30 min. As shown in Fig. 3, poly(I:C) bound to iDCs and HEK293 cells in a dose-dependent manner. The extent of poly(I:C) binding depended on the cell type and on the individual cells in the case of iDCs. In contrast, in vitro-transcribed dsRNAs hardly bound to iDCs and HEK293 cells.

CpG ODNs but not synthetic TLR7/8 ligands inhibit poly(I:C)-induced IFN-β production in mDCs

Previous studies demonstrated that CpG ODNs are endocytosed into mice bone marrow-derived DCs (31, 32). To examine the effects of nucleic acids on poly(I:C)-induced IFN-β production, inhibition analysis was performed using synthetic ligands of TLR7, 8, and 9. iDCs were preincubated with increasing concentrations of nucleic acids for 1 h and then stimulated with poly(I:C). The TLR7/8 ligands, i.e., Imiquimod, Gardiquimod, and CL075, did not affect poly(I:C)-induced IFN-β production (Fig. 4*A*, data not shown). In contrast, the TLR9 ligands, i.e., CpG ODNs, inhibited poly(I:C)-induced IFN-β production in iDCs (Fig. 4*B*). Both B-type ODN2206 and C-type ODN M362 that induce IL-6 production and B cell proliferation completely inhibited poly(I:C)-induced IFN-β production in the 1 to 10 μg/ml range, while A-type

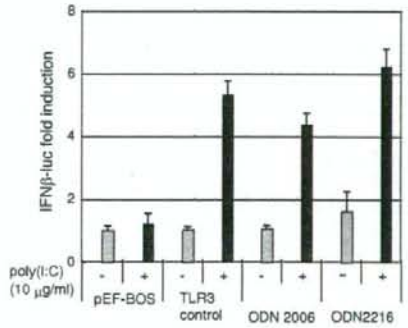

FIGURE 6. ODNs do not affect poly(I:C) recognition by endosomal TLR3. HEK293 cells in 24-well plates were transfected with pEFBOS/hTLR3 together with the reporter plasmid. Twenty-four hours after transfection, the cells were washed and stimulated with poly(I:C) (0.5 μg) and ODN2006 or ODN2216 (0.5 μg) complexed with DOTAP. After 6 h, the luciferase reporter activities were measured. Representative data from a minimum of three separate experiments are shown.

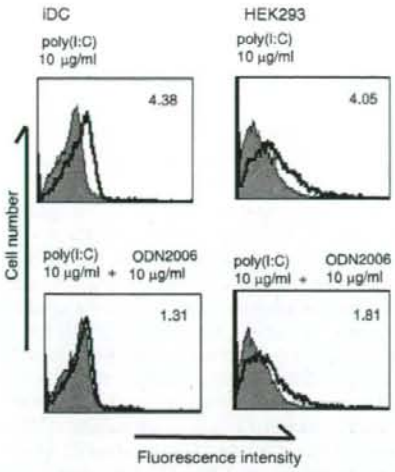

FIGURE 7. ODN2006 competes for surface binding with poly(I:C). Monocyte-derived iDCs and HEK293 cells were incubated with 10 μg/ml poly(I:C) in the presence or absence of 10 μg/ml ODN2006 for 30 min at 4°C. After washing, cells were stained with anti-dsRNA mAb (solid line) or control mouse IgG2a (shaded histograms) for 30 min at 4°C and then FITC-labeled secondary Ab. Inset values indicate the mean fluorescent intensities specific for the anti-dsRNA mAb.

ODN2216 that induces robust IFN-α production in plasmacytoid DCs (pDCs) retarded poly(I:C) function in a dose-dependent manner (Fig. 4*B*). In addition, control ODN2006, a non-TLR9 ligand, also completely inhibited poly(I:C)-induced IFN-β production in a manner similar to that of ODN2006 (Fig. 4*B*), indicating that the inhibitory effect of the ODNs appears to depend on their specific sequences, not on their immunostimulatory features. In the 1 to 100 ng/ml range, ODN2006, ODN M362, and control ODN2006 inhibited poly(I:C)-induced IFN-β production in a dose-dependent manner (Fig. 4*C*). Since 10 μg/ml poly(I:C) (approximate length, 1500 bps) and 67 ng/ml ODN2006 each correspond to 8 pmol/ml, it is possible that poly(I:C) competes with ODNs for binding to a cell surface molecule that mediates endocytosis.

In contrast, the inhibitory effects of ODNs on poly(I:C)-induced TLR3 signaling in TLR3-expressing HEK293 cells were somewhat different from those in iDCs. In the 2 to 50 μg/ml range, B-type ODN2006 and C-type ODN M362 inhibited poly(I:C)-induced IFN-β promoter activation in a dose-dependent manner, while A-type ODN2216 did not affect the poly(I:C) function (Fig. 5). In TLR3-expressing HEK293 cells, it is possible that some TLR3 molecules that were present on the cell surface contribute to poly(I:C) internalization in conjunction with the uptake receptor.

Poly(I:C) recognition by endosomal TLR3 in the presence of ODNs

The inhibitory effect of ODN2006 on poly(I:C)-induced IFN-β production was abrogated when the cells were washed after preincubation with ODNs and then stimulated with poly(I:C) (data not shown). It is necessary for ODNs and poly(I:C) to be present together to inhibit poly(I:C) function. To rule out the possibility that ODNs affect TLR3-mediated poly(I:C) recognition by forming a complex with poly(I:C), poly(I:C) was introduced into the endosomal compartment together with ODNs by using DOTAP, and IFN-β production or promoter activation was measured. As shown in Fig. 6, poly(I:C) induced IFN-β promoter activation through TLR3 regardless of whether the ODNs were present or absent.

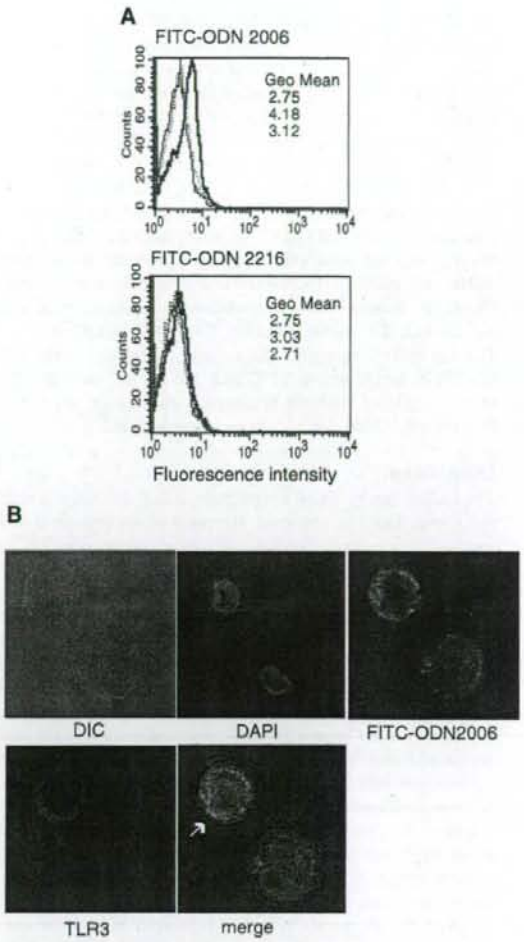

FIGURE 8. ODN2006 shares the uptake receptor with poly(I:C). *A*, Flow cytometric analysis of ODNs uptake by DCs. Monocyte-derived iDCs were incubated with FITC-ODNs (8 pmol/ml) in the presence or absence of an equal molar concentration of poly(I:C) for 2 h at 37°C. *Upper panel*, Binding and internalization of B-type ODN2006; *Lower panel*, Binding and internalization of A-type ODN2216. Black lines show self-fluorescence of the cells. Red and green lines represent the fluorescence of FITC-ODNs that are bound and endocytosed in the absence and presence of poly(I:C), respectively. Mean fluorescent intensities are shown. *B*, Confocal images of FITC-ODN2006 that has been taken up in iDCs and those of endogenous TLR3 in iDCs. iDCs were incubated with 2 μM FITC-ODN2006 for 30 min at 37°C. After washing, the cells were fixed and endogenous TLR3 was stained with anti-TLR3 mAb (TLR3.7) followed by Alexa568-labeled anti-mouse IgG. Nuclei were stained with DAPI (blue color). Green: ODN2006, Red: TLR3, Yellow: merged. Arrow indicates the colocalization of ODN2006 and TLR3. Faint TLR3 staining was observed in the lower right-hand iDC.

These results imply that ODNs inhibit poly(I:C) function during the binding and uptake processes.

ODN2006 shares the uptake receptor with poly(I:C)

To test the possibility that B- and C-type ODN compete for surface binding with poly(I:C), iDCs and HEK293 cells were incubated with poly(I:C) in the presence or absence of ODN2006 for 30 min

at 4°C. The binding of poly(I:C) on the cell surface was assessed by flow cytometry with anti-dsRNA mAb and FITC-labeled secondary Ab. The poly(I:C) binding level was reduced in the presence of ODN2006 in both iDCs and HEK293 cells (Fig. 7). Similar results were obtained with ODNM362 (data not shown). We next analyzed the binding and internalization of FITC-labeled ODNs in iDCs by using flow cytometry. The binding and internalization of FITC-ODN2006 was observed in iDCs, and this was markedly reduced in the presence of poly(I:C) (Fig. 8*A*, *upper panel*). In contrast, FITC-labeled ODN2216 hardly bound to iDCs (Fig. 8*A*, *lower panel*), suggesting that an unknown membrane receptor mediates cell entry of ODN2006 and poly(I:C) but not that of ODN2216. Similar results were obtained with HEK293 cells (data not shown). To examine whether ODN2006 is delivered to the TLR3-positive organelle, iDCs were incubated with FITC-ODN2006 for 30 min at 37°C and then stained with anti-TLR3 mAb. Cells were analyzed by confocal microscopy. As shown in Fig. 8*B*, ODN2006 partly colocalized with TLR3.

Discussion

The mechanism by which exogenously added dsRNA can activate endosomal TLR3 is unknown. By using pharmacological inhibitors, we demonstrated that the clathrin-dependent endocytic pathway participates in dsRNA-mediated TLR3 activation. Among the synthetic dsRNAs, poly(I:C) is preferentially internalized and activates TLR3 in monocyte-derived iDCs resulting in potent IFN-β induction. In vitro transcribed MV-originated dsRNA hardly activates TLR3 when iDCs are stimulated extracellularly. Putative RNA capture at the cell surface may involve the binding and transfer of poly(I:C) but not that of MV-originated synthetic dsRNA. In addition, B- and C-type ODNs compete with poly(I:C) for cellular uptake and inhibit poly(I:C)-induced IFN-β production in iDCs in a dose-dependent manner. This indicates that in mDCs, the uptake receptor is shared by poly(I:C) and B- and C-type ODNs.

Lee et al. (16) reported that CD14 directly bound poly(I:C) small fragments and mediated the cellular uptake of poly(I:C) small fragments in mice bone marrow-derived macrophages. In the human fibroblast cell line MRC5, which expresses TLR3 and CD14 on the cell surface, poly(I:C)-induced IFN-β production was inhibited by pretreatment of the cells with chloroquine (M. Matsumoto, S. Okahira, and T. Seya, unpublished data). Anti-human TLR3 mAb (TLR3.7) inhibits poly(I:C)-induced IFN-β production in MRC5 cells, indicating that cell-surface TLR3 might be involved in poly(I:C) recognition (5). Furthermore, surface expression of both TLR3 and CD14 was decreased 30 min after poly(I:C) stimulation (M. Matsumoto, unpublished data), suggesting that CD14 and TLR3 participate in poly(I:C) uptake in human fibroblasts. In contrast, monocyte-derived iDCs and HEK293 cells do not express CD14 (19). Thus, another cell surface molecule must be involved in the cellular uptake of poly(I:C) in both cell types.

Our results showed that poly(I:C)-induced IFN-β production in iDCs was inhibited only when ODNs were also present and that the synthetic ligands for TLR7/8 did not inhibit this production (Fig. 4). Since TLR9 was not expressed on human mDCs (data not shown and Ref. 33), it is unlikely that the inhibitory effect of ODNs is caused by TLR9-mediated signaling. Additionally, all types of ODNs did not affect poly(I:C)-mediated IFN-β production when poly(I:C) and ODNs were delivered to endosomal compartments with DOTAP (Fig. 6). Finally, surface binding of poly(I:C) was reduced in the presence of B- and C-type ODNs (Fig. 7 and data not shown) and also, binding and internalization of FITC-labeled ODN2006 (type B) was decreased in the presence of an equimolar concentration of poly(I:C) (Fig. 8*A*). These results suggest that poly(I:C) shares the uptake receptor with B- and C-type ODNs in iDCs and that the inhibitory effects of B- and C-type ODNs rely on competitive binding between poly(I:C) and B- and C-type ODNs to the cell-surface receptor. In contrast, the binding and internalization of A-type ODN2216 was hardly observed in iDCs. A-type CpG ODNs (CpG-A) are potent IFN-α inducers in pDCs (34, 35). TLR9 activation by CpG-A occurs in the early endosome and leads to IFN-α production, whereas B-type CpG ODNs (CpG-B) localize to the lysosome and promote pDCs maturation (31, 32). In contrast, both CpG-A and CpG-B are delivered to the lysosome in mouse conventional DCs that express TLR9 intracellularly (31). These results imply that CpG-A and CpG-B are endocytosed through different cell surface receptors and pDCs possess specific machinery that retains the uptake receptor for CpG-A into the early endosome. In human monocyte-derived iDCs, the uptake receptor for A-type ODNs is hardly expressed, suggesting that the expression patterns of uptake receptors differ between human and mouse cells. The inhibitory effect of ODN2216 observed at excess concentrations in iDCs may reflect the weak affinity of A-type ODNs to the poly(I:C) uptake receptor.

It has been shown that poly(I:C) is delivered to the late endosome and then to the lysosome in CHO cells (16). In contrast to TLR9-MyD88 signaling, it appears that TLR3-TICAM-1 signaling does not require endosomal retention of poly(I:C). Once endosomal TLR3 is activated by poly(I:C), an adaptor molecule TICAM-1 transiently colocalizes with TLR3 and then dissociates from the receptor and forms the TICAM-1 signalosome (36). We have observed the colocalization of FITC-labeled ODN2006 and TLR3 in iDCs, indicating that the intracellular trafficking of poly(I:C) and ODN2006 is the same.

Natural and synthetic TLR7 ligands inhibit CpG-A- and CpG-C-ODN-induced IFN-α production in human pDCs (37). The TLR7 signal appears to regulate the outcome of TLR7 ligand/CpG-A-ODN costimulation. Although human mDCs express TLR8, the synthetic TLR8 ligand CL075 did not induce IFN-β production; further it did not affect poly(I:C)-induced IFN-β production in iDCs (Fig. 4*B*). Similar results were obtained with TLR3-expressing HEK293 cells and from the reporter assay for IFN-β promoter activation. The mechanisms by which extracellular TLR7/8 ligands are delivered to intracellular TLR7/8 may differ from those of TLR3/9.

Our data clearly demonstrated that mDCs possess the uptake receptor for poly(I:C) but not that for in vitro-transcribed dsRNA. B- and C-type ODNs share the internalization receptor with poly(I:C). Both poly(I:C) and ODNs are synthetic nucleic acids that do not represent natural virus products, and there are no common structural motifs. The molecular structure of nucleic acids required for recognition by the cell surface receptor should be different from that required for TLR3 activation. It is important to investigate whether virus-derived RNA activates TLR3 extracellularly. TLR3-mediated mDCs activation results in the production of IL-12p70 and IFN-α/β and DC maturation that in turn activates NK cells and CTL (38, 39). At least in mDCs in which TLR3 is localized intracellularly, the ligand properties recognized by the catch-up receptor are critical for TLR3 activation. Identification of virus-derived RNA that is recognized by both the catch-up receptor and TLR3 would clarify the in vivo function of TLR3 during viral infection.

Acknowledgments

We thank Drs. T. Ebihara, H. Oshiumi, M. Shingai, M. Sasai, and A. Matsuo in our laboratory for valuable discussions and H. Itoh for providing the materials. We also thank Dr. T. Taniguchi (University of Tokyo, Japan) and Dr. S. Nishikawa (Institute for Biological Resource and Function, Tsukba, Japan) for providing the reagents.

Disclosures

The authors have no financial conflict of interest.

References

1. Muller, U., U. Steinhoff, L. F. Reis, S. Hemmi, J. Pavlovic, R. M. Zinkernagel, and M. Aguet. 1994. Functional role of type I and type II interferons in antiviral defense. *Science* 264: 1918–1921.
2. Stetson, D., and R. Medzhitov. 2006. Type I interferons in host defense. *Immunity* 25: 373–381.
3. Levy, D. E. 2002. Whence interferon? Variety in the production of interferon in response to viral infection. *J. Exp. Med.* 195: F15–F18.
4. Alexopoulou, L., A. C. Holt, R. Medzhitov, and R. A. Flavell. 2001. Recognition of double stranded RNA and activation of NF-κB by Toll-like receptor 3. *Nature* 413: 732–738.
5. Matsumoto, M., S. Kikkawa, M. Kohase, K. Miyake, and T. Seya. 2002. Establishment of monoclonal antibody against human Toll-like receptor 3 that blocks double-stranded RNA-mediated signaling. *Biochem. Biophys. Res. Commun.* 293: 1364–1369.
6. Yoneyama, M., M. Kikuchi, T. Natsukawa, N. Shinobu, T. Imaizumi, M. Miyagishi, K. Taira, S. Akira, and T. Fujita. 2004. The RNA helicase RIG-I has an essential function in double-stranded RNA-induced innate antiviral responses. *Nat. Immunol.* 5: 730–737.
7. Yoneyama, M., M. Kikuchi, K. Matsumoto, and T. Fujita. 2004. Shared and unique functions of the DExD/H-box helicases RIG-I, MDA5, and LGP2 in antiviral innate immunity. *J. Immunol.* 175: 2851–2858.
8. Kato, H., O. Takeuchi, S. Sato, M. Yoneyama, M. Yamamoto, K. Matsui, S. Uematsu, A. Jung, T. Kawai, K. J. Ishii, et al. 2006. Differential roles of MDA5 and RIG-I helicases in the recognition of RNA viruses. *Nature* 441: 101–105.
9. Gitlin, L., W. Barchet, S. Gilfillan, M. Cella, B. Beutler, R. A. Flavell, M. S. Diamond, and M. Colona. 2006. Essential role of mda-5 in type I IFN responses to polyriboinosinic:polyribocytidylic acid and encephalomyocarditis picornavirus. *Proc. Natl. Acad. Sci. USA* 103: 8459–8464.
10. Matsumoto, M., K. Funami, M. Tanabe, H. Oshiumi, M. Shingai, Y. Seto, M. Yamamoto, and T. Seya. 2003. Subcellular localization of Toll-like receptor 3 in human dendritic cells. *J. Immunol.* 171: 3154–3162.
11. Funami, K., M. Matsumoto, H. Oshiumi, T. Akazawa, A. Yamamoto, and T. Seya. 2004. The cytoplasmic "linker region" in Toll-like receptor 3 controls receptor localization and signaling. *Int. Immunol.* 16: 1143–1154.
12. Oshiumi, H., M. Matsumoto, K. Funami, T. Akazawa, and T. Seya. 2003. TICAM-1, an adaptor molecule that participates in Toll-like receptor 3-mediated interferon-β induction. *Nat. Immunol.* 4: 161–167.
13. Yamamoto, M., S. Sato, H. Hemmi, K. Hoshino, T. Kaisho, H. Sanjo, O. Takeuchi, M. Sugiyama, M. Okabe, K. Takeda, and S. Akira. 2003. Role of adaptor TRIF in the MyD88-independent Toll-like receptor signaling pathway. *Science* 301: 640–643.
14. Takada, E., S. Okahira, M. Sasai, K. Funami, T. Seya, and M. Matsumoto. 2007. C-terminal LRRs of human Toll-like receptor 3 control receptor dimerization and signal transmission. *Mol. Immunol.* 44: 3633–3640.
15. Leonard, J. N., R. Ghirlando, J. Askins, J. K. Bell, D. H. Margulies, D. R. Davies, and D. M. Segal. 2008. The TLR3 signaling complex forms by cooperative receptor dimerization. *Proc. Natl. Acad. Sci. USA* 105: 258–263.
16. Lee, H. K. S., K. Dunzendorfer, K. Soldau, and P. S. Tobias. 2006. Double-stranded RNA-mediated TLR3 activation is enhanced by CD14. *Immunity* 24: 153–163.
17. Akashi, S., S. Saiyoh, Y. Wakabayashi, T. Kikuchi, N. Takamura, Y. Nagai, Y. Kusumoto, K. Fukase, S. Kusumoto, Y. Adachi, et al. 2003. Lipopolysaccharide interaction with cell surface Toll-like receptor 4-MD-2: higher affinity than that with MD-2 or CD14. *J. Exp. Med.* 198: 1035–1042.
18. Manukyan, M., K. Triantafilou, M. Triantafilou, A. Mackie, N. Nilsen, T. Espevik, K. H. Wiesmuller, A. J. Ulmer, and H. Heine. 2005. Binding of lipopeptide to CD14 induces physical proximity of CD14, TLR2 and TLR1. *Eur. J. Immunol.* 35: 911–921.
19. Tsuji, S., M. Matsumoto, O. Takeuchi, S. Akira, I. Azuma, A. Hayashi, K. Toyoshima, and T. Seya. 2000. Maturation of human dendritic cells by cell wall skeleton of *Mycobacterium bovis* bacillus Calmette-Guérin: involvement of toll-like receptors. *Infect. Immun.* 68: 6883–6890.
20. Schönborn, J., J. Oberstrass, E. Breyel, J. Tittgen, J. Schumacher, and N. Lukacs. 1991. Monoclonal antibodies to double-stranded RNA as probes of RNA structure in crude nucleic acid extracts. *Nucleic Acids Res.* 19: 2993–3000.
21. Okahira, S., F. Nishikawa, S. Nishikawa, T. Akazawa, T. Seya, and M. Matsumoto. 2005. Interferon-β induction through Toll-like receptor 3 depends on double-stranded RNA structure. *DNA Cell Biol.* 24: 614–623.
22. Hornung, V., J. Ellegast, S. Kim, K. Brzózka, A. Jung, H. Kato, H. Poeck, S. Akira, K.-K. Conzelmann, M. Schlee, et al. 2006. 5′-Triphosphate RNA is the ligand for RIG-I. *Science* 314: 994–997.
23. Puri, V., R. Watanabe, R. D. Singh, M. Dominguez, J. C. Brown, C. L. Wheatly, D. L. Marks, and R. E. Pagano. 2001. Clathrin-dependent and -independent internalization of plasma membrane sphingolipids initiates two Golgi targeting pathways. *J. Cell Biol.* 154: 535–547.
24. Sieczkarski, S. B., and G. R. Whittaker. 2002. Dissecting virus entry via endocytosis. *J. Gen. Virol.* 83: 1535–1545.
25. Saleh, M. C., R. P. van Rij, A. Hekele, A. Gillis, E. Foley, P. H. O'Farrell, and R. Andino. 2006. The endocytic pathway mediates cell entry of dsRNA to induce RNAi silencing. *Nat. Cell Biol.* 8: 793–802.
26. Okamoto, Y., H. Ninomiya, S. Miwa, and T. Masaki. 2000. Cholesterol oxidation switches the internalization pathway of endothelin receptor type A from caveolae to clathrin-coated pits in Chinese hamster ovary cells. *J. Biol. Chem.* 275: 6439–6446.
27. Zhang, Y., A. M. Ahmed, N. McFarlane, C. Capone, D. R. Boreham, R. Truant, S. A. Igdoura, and B. L. Trigatti. 2007. Regulation of SR-BI-mediated selective lipid uptake in Chinese hamster ovary-derived cells by protein kinase signaling pathways. *J. Lipid Res.* 48: 405–416.
28. Orlandi, P. A., and P. H. Fishman. 1998. Filipin-dependent inhibition of cholera toxin: evidence for toxin internalization and activation through caveolae-like domains. *J. Cell Biol.* 141: 905–915.
29. Peiser, L., S. Mukhopadhyay, and S. Gordon. 2002. Scavenger receptors in innate immunity. *Curr. Opin. Immunol.* 14: 123–128.
30. Marshall-Clarke, S., J. E. Downes, I. R. Haga, A. G. Bowie, P. Borrow, J. L. Pennock, R. K. Grencis, and P. Rothwell. 2007. Polyinosinic acid is a ligand for toll-like receptor 3. *J. Biol. Chem.* 282: 24759–24766.
31. Honda, K., Y. Ohba, H. Yanai, H. Negishi, T. Mizutani, A. Takaoka, C. Taya, and T. Taniguchi. 2005. Spatiotemporal regulation of MyD88-IRF7 signaling for robust type I-interferon induction. *Nature* 434: 1035–1040.
32. Guiducci, C., G. Ott, J. H. Chan, E. Damon, C. Calacsan, T. Matray, K. D. Lee, R. L. Coffman, and F. J. Barrat. 2006. Properties regulating the nature of the plasmacytoid dendritic cell response to Toll-like receptor 9 activation. *J. Exp. Med.* 203: 1999–2008.
33. Kadowaki, N., S. Ho, S. Antonenko, R. W. Malefyt, R. A. Kastelein, F. Bazan, and Y. J. Liu. 2001. Subsets of human dendritic cell precursors express different Toll-like receptors and respond to different microbial antigens. *J. Exp. Med.* 194: 863–869.
34. Krieg, A. M. 2002. CpG motifs in bacterial DNA and their immune effects. *Annu. Rev. Immunol.* 20: 709–760.
35. Stunz, L. L., P. Lenert, D. Peckham, A. K. Yi, S. Haxhinasto, M. Chang, A. M. Krieg, and R. F. Ashman. 2002. Inhibitory oligonucleotides specifically block effects of stimulatory CpG oligonucleotides in B cells. *Eur. J. Immunol.* 32: 1212–1222.
36. Funami, K., M. Sasai, Y. Ohba, H. Oshiumi, T. Seya, and M. Matsumoto. 2007. Spatiotemporal mobilization of Toll-IL-1 receptor domain-containing adaptor molecule-1 in response to dsRNA. *J. Immunol.* 179: 6867–6872.
37. Berghofer, B., G. Haley, T. Frommer, G. Bein, and H. Hackstein. 2007. Natural and synthetic TLR7 ligands inhibit CpG-A- and CpG-C-oligodeoxynucleotide-induced IFN-α production. *J. Immunol.* 178: 4072–4079.
38. Schultz, O., S. S. Diebold, M. Chen, T. Naslund, M. A. Nolte, L. Alexopoulou, Y.-T. Azuma, R. A. Flavell, P. Liljestrom, and C. R. Sousa. 2005. Toll-like receptor 3 promotes cross-priming to virus-infected cells. *Nature* 433: 887–892.
39. Akazawa, T., T. Ebihara, M. Okuno, Y. Okuda, M. Shingai, K. Tsujimura, T. Takahashi, M. Ikawa, M. Okabe, N. Inoue, et al. 2007. Antitumor NK activation induced by the TLR3-TICAM-1 (TRIF) pathway in myeloid dendritic cells. *Proc. Natl. Acad. Sci. USA* 104: 252–257.

THE JOURNAL OF BIOLOGICAL CHEMISTRY VOL. 283, NO. 43, pp. 28835–28841, October 24, 2008

Mycolyltransferase-mediated Glycolipid Exchange in Mycobacteria*

Received for publication, July 28, 2008, and in revised form, August 14, 2008 Published, JBC Papers in Press, August 14, 2008, DOI 10.1074/jbc.M805776200

Isamu Matsunaga[‡§], Takashi Naka[¶], Rahul S. Talekar[‖], Matthew J. McConnell[‖], Kumiko Katoh[‡§], Hitomi Nakao[‡§], Atsushi Otsuka[‡], Samuel M. Behar[‖], Ikuya Yano[¶], D. Branch Moody[‖], and Masahiko Sugita[‡§1]

From the [‡]Laboratory of Cell Regulation, Institute for Virus Research and [§]Laboratory of Cell Regulation and Molecular Network, Graduate School of Biostudies, Kyoto University, Kyoto 606-8507, Japan, [¶]Japan BCG Laboratory, Tokyo 204-0022, Japan, and [‖]Division of Rheumatology, Immunology, and Allergy, Brigham and Women's Hospital, Harvard Medical School, Boston, Massachusetts 02115

Trehalose dimycolate (TDM), also known as cord factor, is a major surface glycolipid of the cell wall of mycobacteria. Because of its potent biological functions in models of infection, adjuvancy, and immunotherapy, it is important to determine how its biosynthesis is regulated. Here we show that glucose, a host-derived product that is not readily available in the environment, causes *Mycobacterium avium* to down-regulate TDM expression while up-regulating production of another major glycolipid with immunological roles in T cell activation, glucose monomycolate (GMM). *In vitro*, the mechanism of reciprocal regulation of TDM and GMM involves competitive substrate selection by antigen 85A. The switch from TDM to GMM biosynthesis occurs near the physiological concentration of glucose present in mammalian hosts. We further demonstrate that GMM is produced *in vivo* by mycobacteria growing in mouse lung. These results establish an enzymatic pathway for GMM production. More generally, these observations provide a specific enzymatic mechanism for dynamic alterations of cell wall glycolipid remodeling in response to the transition from noncellular to cellular growth environments, including factors that are monitored by the host immune system.

Mycobacterium avium complex (MAC)[2] includes a group of acid-fast bacteria that distribute widely in natural environments, including soil, water, aerosols, and dust (1). Although less virulent than *Mycobacterium tuberculosis*, these environmental mycobacteria occasionally infect humans, especially patients infected with human immunodeficiency virus type 1, where they represent a major cause of morbidity. The incidence of clinically overt MAC infection has increased significantly in recent years, and because of the multidrug resistance evolved by the microbes, MAC infection is difficult to clear with chemotherapeutic agents. Thus, *M. tuberculosis* and MAC are now the two major groups of mycobacteria species that require further efforts for prevention and treatment. Unlike *M. tuberculosis*, which transmits primarily from individuals with active disease, epidemiologic evidence suggests that such transmission pathways are unlikely for MAC. Rather, MAC infection appears to occur when susceptible individuals are exposed to environmental MAC. These observations predict that, upon infection, environmental MAC should undergo significant adaptive changes to allow its survival and replication within the host.

Mycobacteria possess highly lipid-rich cell walls that are critical not simply for their acid-fast properties but also for their survival and replication. The cell wall contains mycolic acids, an α-alkyl-β-hydroxy fatty acid with extremely long carbon chains ($\sim C_{80}$), which are densely aligned in covalent association with the 6-position of arabinose termini of the underlying arabinogalactan sugar layer or exist as free molecules complexed to sugars, either glucose or trehalose. Arabinogalactan-linked mycolates are proposed to extend outward and interact noncovalently with carbon chains of the so-called surface-exposed glycolipids, including trehalose 6-monomycolate (TMM), trehalose 6,6′-dimycolate (TDM), and glucose 6-monomycolate (GMM), thereby forming the hydrophobic cell wall architecture that is essential for protection against chemical attack, such as reactive oxygen intermediates and hydrolytic enzymes derived from the host cells. Among the most abundant surface-exposed glycolipids is TDM that is biosynthesized from its precursor, TMM, by the mycolyltransferase activity of antigen 85 (Ag85) (2). Many biological functions have been assigned to TDM (3) that may impact on survival of mycobacteria within the host and possibly their virulence. Therefore, it is important to determine how biosynthesis of TDM and other mycolic acid-containing glycolipids is regulated by external factors. GMM exists at varied levels in the mycobacterial cell wall (4, 5). In addition to its role in cell wall barrier functions, GMM is a granuloma-forming agent in mice (6) as well as a CD1b presented antigen in humans (7).

* This work was supported, in whole or in part, by National Institutes of Health Grant R01 07155 (NIAID) (to D. B. M.). This work was also supported by grants-in-aid from scientific research on priority areas from the Ministry of Education, Culture, Sports, Science and Technology (to M. S.), grants-in-aid for scientific research B (to M. S.) and C (to I. M.) from the Japan Society for the Promotion of Science, grants from the Ministry of Health, Labour, and Welfare Research on Emerging and Re-emerging Infectious Diseases (to M. S.), and by the Burroughs Wellcome Fund (to D. B. M.). The costs of publication of this article were defrayed in part by the payment of page charges. This article must therefore be hereby marked "*advertisement*" in accordance with 18 U.S.C. Section 1734 solely to indicate this fact.

The nucleotide sequence(s) reported in this paper has been submitted to the DDBJ/GenBank™/EBI Data Bank with accession number(s) AB325677.

[1] To whom correspondence should be addressed: 53 Kawahara-cho, Shogoin, Sakyo-ku, Kyoto 606-8507, Japan. Fax: 81-75-752-3232; E-mail: msugita@virus.kyoto-u.ac.jp.

[2] The abbreviations used are: MAC, *Mycobacterium avium* complex; Ag85, antigen 85; GC-MS, gas chromatography-mass spectrometry; GMM, glucose 6-monomycolate; IL-2, interleukin-2; MALDI-TOF MS, matrix-assisted laser desorption ionization-time of flight mass spectrometry; TCR, T cell receptor; TDM, trehalose 6,6′-dimycolate; TMM, trehalose 6-monomycolate; LC-MS, liquid chromatography-mass spectrometry.

Here we identify Ag85A as an enzyme that produces GMM by transfer of mycolate to glucose. Furthermore, mechanistic studies show that glucose present in its growth environment regulates the spectrum of mycolylglycolipids made by MAC, and glucose from the host influences GMM production *in vivo* during infection of mice. Mechanistic studies showed that glucose and trehalose compete as substrates for Ag85A, linking the biosynthesis pathways of GMM and TDM.

EXPERIMENTAL PROCEDURES

Reagents and Bacteria—Chemical reagents were purchased from Nacalai Tesque (Kyoto, Japan) unless otherwise indicated. *M. avium* ATCC 35767 (serovar 4) was obtained from American Type Culture Collection (Manassas, VA). The bacteria were maintained on a plate of Middlebrook 7H10 media supplemented with 10% oleic acid/albumin/dextrose/catalase (BD Biosciences). For extraction of the total lipid fraction, the bacteria were cultured in Middlebrook 7H9 broth media (containing 0.05% Tween 80 but not glycerol) supplemented with 10% albumin/dextrose/catalase (BD Biosciences). The log phase culture was diluted with 20 volumes of 7H9 media containing various concentrations of glucose, and the culture was continued for another 5–7 days until the absorbance at 600 nm reached ~1. In some experiments, bacteria were grown in media containing either 0.01 or 0.1% glucose, and the media were replaced every day with fresh media containing the same concentrations of glucose. After 5 days, the bacteria were harvested for lipid extraction. To monitor early GMM production, bacteria were grown either in 7H9 media containing 0.01 or 0.1% glucose or in human serum and were harvested after 2, 4, 8, 18, and 24 h of culture.

Preparation of Mycolylglycolipids from MAC—Total lipids from mycobacteria were prepared as described previously (8). The total lipids were then dissolved in chloroform/methanol (C/M, 2:1, v/v), and 20 volumes of ice-cold acetone were added. After 30 min of incubation on ice, the suspension was subjected to centrifugation at 1,500 × *g* for 15 min at 1 °C, and the supernatant was carefully removed. The pellet was then washed with ice-cold acetone, and the residue was dissolved in C/M (2:1) and fractionated by TLC using an Analtech TLC plate (Newark, DE) with a solvent system of chloroform/methanol/acetone/acetic acid (90:10:10:1, v/v). GMM, TDM and TMM fractions were extracted with C/M (2:1) from the silica gels. For GMM and TDM purification, the fractions were further fractionated by TLC with a solvent system of chloroform/acetone/methanol/water (50:60:2.5:0.6, v/v). Finally, the GMM, TDM and TMM fractions were extracted with C/M (2:1), dried, and rinsed several times with methanol at room temperature to remove any residual contamination of glycopeptidolipids and phospholipids.

Matrix-assisted Laser Desorption Ionization-Time of Flight Mass Spectrometry (MALDI-TOF MS)—MALDI-TOF MS analyses of glycolipids were carried out according to the method described previously (9). Briefly, MALDI-TOF MS spectra were acquired on a Voyager DE-STR MALDI-TOF mass spectrometer (Applied Biosystems) with a pulse laser emitting at 337 nm. Samples were analyzed in the reflectron mode with an accelerating voltage operating in positive ion mode of 20 kV. As the matrix, 2,5-dihydroxybenzoic acid was used.

Gas Chromatography-Mass Spectrometry (GC-MS)—GC-MS analysis of the sugar moiety of GMM was carried out according to the method described previously (9). Briefly, GMM was hydrolyzed with 2 M trifluoroacetic acid at 120 °C for 2 h. The aqueous phase was dried, reduced with 10 mg/ml solution of $NaBD_4$ (1 M NH_4OH/C_2H_5OH, 1:1, v/v) at room temperature for 2 h, and then acetylated with acetic anhydride/pyridine (1:1, v/v) at 100 °C for 1 h. The resulting alditol acetate derivatives were analyzed by GC-MS with GCMS-QP2010 plus (Shimazu Co., Ltd., Kyoto, Japan), using a fused silica capillary column (SP-2380, 30 m × 0.25 mm inner diameter; Supelco Inc.). GC oven was operated at 50 °C for 0.5 min, and then the temperature was increased to 235 °C at a rate of 65 °C/s. The temperature was then kept at 235 °C for 12 min. Flow rate of helium gas was 44.4 cm/min.

Isolation of the Antigen 85A Gene from MAC, Preparation of the Recombinant Enzyme and Its Enzymatic Assay—The genomic DNA was isolated from the MAC strain using the Isoplant kit according to the manufacturer's instruction (Wako Pure Chemical Co. Ltd., Osaka, Japan). The gene that encoded the mature Ag85A lacking the signal sequence was amplified by PCR, using a specific primer set as follows: 5′-gga att cca tat gtt ctc gcg ccc cgg tct gcc-3′ (a sense primer, in which the NdeI restriction site is underlined) and 5′-ccg ctc gag ggt gcc ctgg ccg ttc ccg g-3′ (an antisense primer, in which the XhoI restriction site is underlined). PCR was carried out using a Takara LA-*Taq*DNA polymerase (Takara Co. Ltd., Tokyo, Japan), and the cycling conditions for PCR amplification were as follows: 94 °C, 2 min, followed by 30 cycles of 98 °C, 20 s and 72 °C, 1.5 min, and a final extension step of 72 °C, 3 min. The amplified PCR products were digested with NdeI and XhoI and ligated to a NdeI-XhoI-digested pET-21c plasmid vector (Merck). The nucleotide sequences of the Ag85A gene were determined for four isolated clones. *Escherichia coli* BL21 (DE3) was transformed with the Ag85A gene in pET-21c, and induction of protein expression was performed according to a method of Kremer *et al.* (10).

The bacteria expressing the His-tagged mature Ag85A were harvested and disrupted by sonication in ice-cold 20 mM Tris-HCl buffer (pH 7.9) containing 0.5 M NaCl and 60 mM imidazole (sonication buffer). The sonicate was centrifuged at 10,000 × *g* for 30 min at 4 °C to remove insoluble materials, and then the supernatant was applied onto a Ni^{2+}-resin column equilibrated with the sonication buffer at 4 °C. After washing the column with the sonication buffer, the recombinant Ag85A was eluted with 20 mM Tris-HCl buffer (pH 7.9) containing 0.5 M NaCl and 0.5 M imidazole. The eluate was concentrated and dialyzed against 50 mM Tris-HCl buffer (pH 7.4) containing 10% glycerol overnight at 4 °C. Protein concentration of the recombinant Ag85A preparation was determined by the Quick Start Bradford protein assay kit (Bio-Rad). Purity of the preparation was determined by SDS-PAGE and Coomassie staining.

Mycolyltransferase assays were carried out by modification of a method of Kremer *et al.* (10). Twenty μg of purified TMM was dispersed by sonication in 150 μl of 50 mM sodium phosphate buffer (pH 7.4) in the presence or absence of indicated

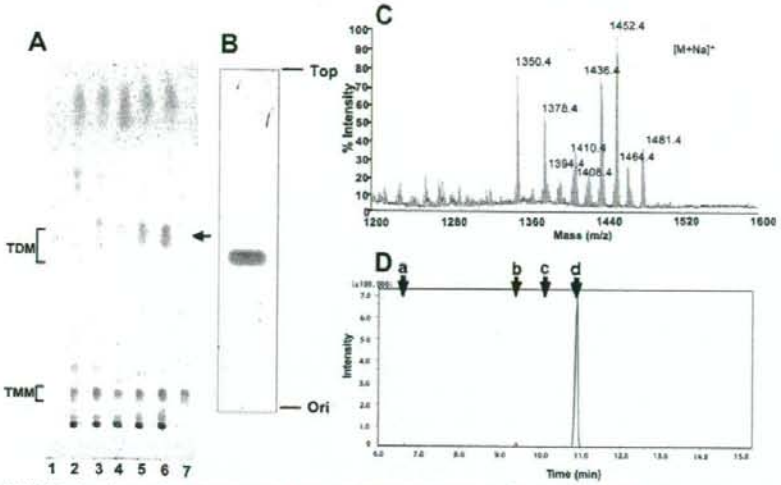

FIGURE 1. **A reciprocal production of TDM and GMM in MAC in response to glucose.** *A*, MAC was cultured in media containing 0.01% (w/v, *lane 2*), 1% (w/v, *lane 3*), 2% (w/v, *lane 4*), 5% (w/v, *lane 5*), and 10% glucose (w/v, *lane 6*), and the total lipid fractions (50 μg each) were analyzed on a TLC plate that was developed with chloroform/methanol/acetone/acetic acid (90:10:10:1, v/v). Purified TDM (*lane 1*) and TMM (*lane 7*) were used as references. Glucose dose-dependent production of a lipid species (indicated with an *arrow*) was detected. *B*, lipid species was purified and analyzed on a silica gel TLC plate that was developed with chloroform/methanol (9:1, v/v). *C*, MALDI-TOF MS profiles of the purified lipid species. *D*, GC-MS analysis of the sugar moiety of the purified lipid species. *Arrows* indicate retention times for the alditol acetate derivatives of arabinose (*a*), mannose (*b*), galactose (*c*)/ and glucose (*d*). Ion chromatogram of *m/z* 290 is shown. The retention time of the major ion corresponded with that of a glucose alditol acetate derivative.

concentration of D-glucose. The reaction was started by the addition of 50 μl of the enzyme preparation containing 50 μg of protein. After 1 h of incubation at 37 °C, the reaction was stopped by the addition of 2 ml of C/M (2:1) and 0.3 ml of distilled water. The lipids were extracted by the method of Kremer *et al.* (10) and analyzed by silica gel TLC. The lipids on the TLC plate were visualized by spraying 50% sulfuric acid and baking.

GMM Detection in Vivo—Mouse infections were carried out via the aerosol route with 10^2 *M. tuberculosis* Erdman strain with mice sacrificed after ~21 days of infection. Lungs were homogenized with beads and centrifuged at 2000 × *g* for 30 min at room temperature. The bacterial pellet was treated with 2% NaOH to disperse phospholipid bilayers, neutralized with 0.27 M phosphoric acid in phosphate buffered saline, and centrifuged at 2000 × *g* for 30 min to recover bacteria. Lipids were extracted from this mixture with three serial extractions in C/M (2:1, 1:1, and 1:2), evaporated to dryness under nitrogen, and resuspended in 1:1 C/M. These lipids were further fractionated by cold acetone precipitation to enrich for lipids that were analyzed by normal phase chromatography on a diol column. Solvent A was methanol, and solvent B was 60:40 (v/v) hexane/2-propanol. Both solvents contained 0.1% (v/v) formic acid and 0.05% (v/v) ammonium hydroxide. A binary gradient was used beginning at 5% solvent A for 3 min, linearly increasing to 40% solvent A over 5 min, holding at 40% solvent A for 6 min, linearly increasing to 100% solvent A over 2.2 min, holding at 100% solvent A for 3 min, linearly decreasing to 5% solvent A over 3.6 min, and finally holding at 5% solvent A for 3.2 min. Compounds matching the expected mass for GMM were detected at after 3.6–3.9 min of elution under these conditions. The accurate mass experiment was carried out with an Agilent 6520 Accurate Mass QTOF-LC-MS operated in the positive mode with an Agilent Technologies 1200 Series high pressure liquid chromatography system. CID-MS was carried out with a ThermoLCQ Advantage Ion Trap mass spectrometer with nano-electrospray ionization in comparison with GMM derived from *Mycobacterium fallax* (11).

GMM-specific T Cell Assays—The T cell receptor (TCR)-deficient Jurkat cells (J.RT3) reconstituted by transfection with GMM-specific, CD1b-restricted TCRs have been described previously (12). The T cells (5×10^4/well) were cocultured in 96-well microtiter plates with the C1R human B-lymphoblastoid cells (1×10^5/well) stably transfected either with CD1b (C1R/CD1b) or with empty vector alone (C1R/mock) (13) in the presence of phorbol 12-myristate 13-acetate (10 ng/ml) and indicated concentrations of lipid preparations. In some experiments, monocyte-derived dendritic cells were used as antigen-presenting cells. After 20 h, aliquots of the culture supernatants were collected, and the amount of interleukin-2 (IL-2) released into the supernatants was measured by the IL-2 ELISA kit (BD Biosciences).

RESULTS

Reciprocal Production of TDM and GMM by MAC in Response to Glucose—Glucose is an essential nutrient to living organisms, which is utilized as a source not only for energy production but also for biosynthesis of glycosylated constituents of cellular architecture. Unlike other hexose sugars, glucose is maintained at high levels in the blood and tissues of mammalian hosts. Therefore, we predicted that, upon infection into the host, MAC grown in glucose-limited environments might undergo significant alterations in glycolipid biosynthesis by exposure to host-derived glucose. To gain insights into the impact of exogenous glucose on glycolipid composition in mycobacteria, we first monitored glycolipid production by *M. avium* strain (serovar 4) that was harvested after cultivation in liquid media supplemented with different concentrations of glucose. The total lipid fraction was obtained by extracting each bacterial preparation with chloroform and methanol. The lipids were then analyzed on a TLC plate developed with a solvent system suitable for separation of chemically diverse glycolipid species (Fig. 1*A*). When grown in the presence of a trace amount of glucose (0.01%, w/v), mycobacteria produced high levels of TDM and TMM (Fig. 1*A*, *lane 2*, shown with *brackets*). As the glucose concentrations present in media were increased,

TDM production decreased, whereas the amount of TMM remained constant (Fig. 1*A*, *lanes 2–6*). Also, an increase in a discrete, unknown lipid species with a retardation factor (R_f) slightly greater than that of TDM was noted (Fig. 1*A*, *lanes 3–6*, indicated with an *arrow*). To determine the molecular identity of the unknown lipid, it was purified and subjected to TLC and MS analyses. The purified lipid was resolved as doublet bands on a TLC plate developed with a solvent system of C/M (9:1, v/v) (Fig. 1*B*). MALDI-TOF MS analysis revealed that the mass numbers of given ions were matched with those of sodium adducts of hexose monomycolate (Fig. 1*C*). Within the limits of error of the method of detection, the masses matched both in terms of the expected *m/z* of the dominant ions, the range of mass variation expected of individual molecular species of mycolate derivatives, and the absolute mass differences among the major ions, which can be accounted for by differences in carbon chain length and substitution of R groups (14). For example, *m/z* 1452.4 corresponds to the expected mass of sodium adduct of hexose monomycolate with C_{85} fatty acid and a wax ester-type R group on the meromycolate chain (Fig. 1*C*). GC-MS analysis of an alditol acetate derivative of the sugar moiety derived from the purified lipid identified glucose as the hexose group attached to mycolates (Fig. 1*D*). The doublet bands observed on a TLC plate were thus likely to represent two stereoisomers of mycolates as described previously (5, 15). Finally, the production of GMM in response to added glucose is expected based on the ability of mycobacteria to couple abundant hexose sugars at mycolyl esters (5). These results detected a reciprocal production of TDM and GMM by MAC in response to exogenous glucose without apparent alterations in the steady state levels of TMM. This experiment, carried out in live bacteria, raised the possibility that mycolyltransferases might compete for carbohydrate substrates.

Ag85 Utilized Glucose for GMM Biosynthesis—Mycobacteria-derived mycolyltransferases, known also as Ag85, catalyze the final step of TDM biosynthesis, using TMM as a substrate. Current models of the Ag85-catalyzed reaction predicted that two molecules of TMM are captured in the two substrate-binding pockets of the enzyme, and the mycolyl acyl group of the TMM substrate bound in one substrate-binding pocket (donor site) is transferred to the other TMM substrate bound in the other pocket (acceptor site), resulting in generation of one molecule of TDM and one molecule of trehalose (Fig. 2*A*) (2, 16). Although GMM can be an abundant structure in the cell wall and functions to activate T cells and form granulomas, its mechanism of synthesis was unknown. We hypothesized that GMM biosynthesis could be catalyzed by Ag85 if glucose, instead of TMM, occupied the acceptor site (Fig. 2*B*). To address this possibility, we made recombinant Ag85A enzyme from the *M. avium* strain (serovar 4), and we performed *in vitro* enzymatic reaction experiments. To accomplish this, we first carried out PCR from the genome of the MAC strain as a template, and isolated the Ag85A gene that encoded the mature protein lacking the signal sequence. DNA sequencing of the isolated gene revealed that three nucleotides were altered as compared with the previously reported Ag85A gene derived from *M. avium* serovar 1 strain (17), but the deduced amino acid sequences were identical in both strains. We then constructed an expression plasmid in which the initiation codon was placed at the 5′-end and the sequence encoding a His tag was attached in frame at the 3′-end of the isolated Ag85A gene. The His-tagged enzyme was expressed in *E. coli* and affinity-purified by Ni^{2+}-charged resin column chromatography. The purified material was resolved as a single band with an apparent molecular mass of ~33 kDa on a Coomassie-stained SDS-polyacrylamide gel, consistent with its being the Ag85A protein (Fig. 3*A*). Incubation of TMM *in vitro* in the presence of this

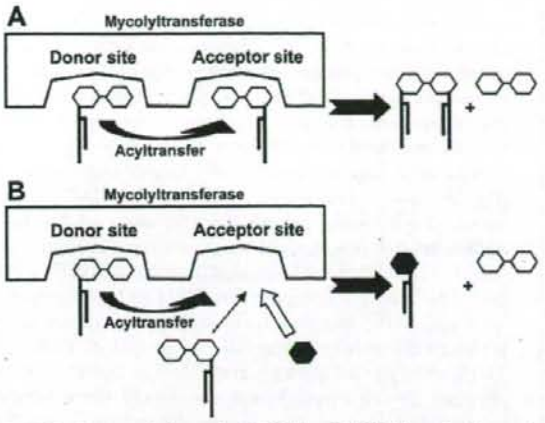

FIGURE 2. **Proposed scheme for TDM (*A*) and GMM (*B*) production catalyzed by mycolyltransferase.** In *model A*, both the donor site and the acceptor site of the enzyme interact with TMM, resulting in TDM formation. In *model B*, a glucose substrate competes against a TMM substrate for access to the acceptor site. When glucose is readily available, glucose rather than TMM preferentially gain access to the site, resulting in production of GMM.

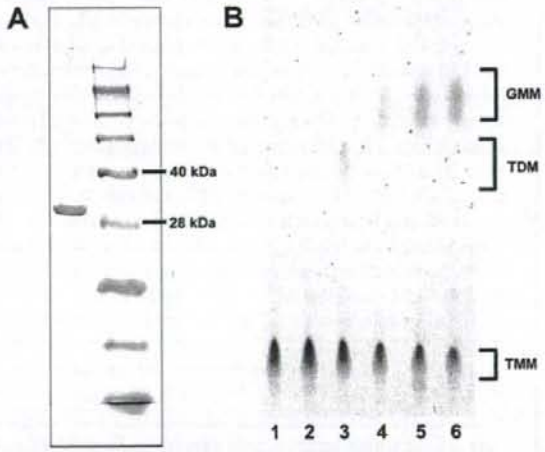

FIGURE 3. **TDM-GMM exchange mediated by recombinant Ag85A.** *A*, purified MAC Ag85A (*left lane*) and a size marker (*right lane*) were resolved on a Coomassie-stained SDS-polyacrylamide gel. Positions for the 40- and 28-kDa marker proteins are indicated. *B*, enzymatic reactions were performed at 37 °C at conditions indicated below, and the lipids were extracted from the reaction mixtures, followed by analysis on a TLC plate. *Lane 1*, Ag85A and TMM with 5% glucose (w/v), 0 h of incubation; *lane 2*, heat-inactivated (100 °C, 3 min) Ag85A and TMM with 5% glucose (w/v), 1 h of incubation; *lanes 3–6*, Ag85A and TMM either with 0.2% (w/v) glucose (*lane 4*), 1% glucose (w/v) (*lane 5*), and 5% (w/v) glucose (*lane 6*) or without glucose (*lane 3*), 1 h of incubation.

enzyme preparation resulted in generation of TDM (Fig. 3*B*, *lane 3*), confirming the mycolyltransferase activity exerted by the recombinant protein. Strikingly, addition of glucose to this reaction condition resulted in decreased TDM production in a dose-dependent manner, which was associated with an increase in GMM (Fig. 3*B*, *lanes 3–6*). GMM synthesis was completely abrogated when heat-inactivated enzyme was used (Fig. 3*B*, *lane 2*). This further confirmed that GMM was produced enzymatically by the mycolyltransferase activity of Ag85A but not as a result of nonenzymatic hydrolysis. These results indicate that Ag85A mediates synthesis of GMM. In this molecular model, we propose that TMM and glucose compete for access to the acceptor site of the Ag85A, and the enzyme preferentially catalyzes biosynthesis of GMM, rather than TDM, when glucose is readily available (Fig. 2*B*). The substrate selection by the mycolyltransferase would likely provide a molecular basis for the glucose-dependent TDM-GMM exchange detected in cultured MAC.

GMM Production Occurs at a Physiological Glucose Concentration—The observations made above have established an enzymatic pathway for GMM production in live mycobacteria that are grown in the presence of high levels of exogenous glucose. However, it remains to be addressed whether mycobacteria can produce GMM under physiological concentrations of glucose present in mammalian hosts, which is maintained at ~100 mg/dl (0.1% w/v). To address this issue, we measured GMM production by mycobacteria cultured in liquid media with a glucose concentration comparable with that in the host. The MAC culture was started in the presence of either 0.01 or 0.1% glucose, and every 24 h, the culture media were replaced with fresh media to maintain the glucose concentrations at constant levels. After 5 days of culture, the bacteria were harvested, and the total lipids were extracted. Subsequently, methanol-insoluble lipids were isolated from these total lipids, followed by separation on TLC plates (Fig. 4*A*). Although TDM production was readily detected in both cultures, GMM production was detected only in the presence of 0.1% glucose (Fig. 4*A*, *lane 2*) but not in the presence of 0.01% glucose (*lane 1*). This was also confirmed by T cell-based assays (Fig. 4*B*) in which Jurkat T cells expressing specific TCRs recognizing GMM in the context of CD1b molecules were used. Incubation of the T cells with CD1b-expressing cells (C1R/CD1b) in the presence of the total lipids from the 0.1% glucose-containing culture resulted in dose-dependent IL-2 production by the T cells, demonstrating high levels of antigenicity when growing at physiological glucose concentrations (Fig. 4*B*, *upper panel*). The specific response was not observed when CD1b-negative cells (C1R/mock) were used as antigen-presenting cells, supporting that the response was CD1b-restricted.

We then addressed how quickly induction of GMM production occurred after exposure to 0.1% glucose. MAC was cultured either in liquid media containing 0.01% (Fig. 5*A*) or 0.1% (*B*) or in human serum (*C*), and the bacteria were harvested at 2, 4, 8, 18, and 24 h. GMM production was observed as early as 8 h after the start of the culture both in 0.1% glucose-containing media and in human serum but not in media containing 0.01% glucose. These observations suggest that GMM production can occur quickly after exposure to high levels of glucose presumably as a result of competitive substrate selection by preexisting mycolyltransferases.

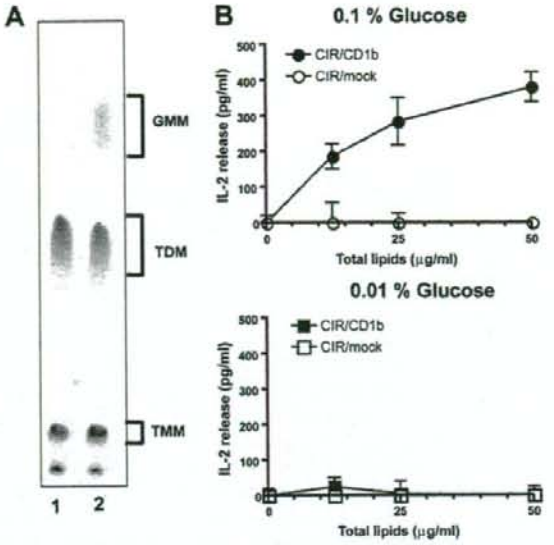

FIGURE 4. **GMM production by mycobacteria cultured at a physiological glucose concentration.** *A*, MAC was cultured in liquid media containing either 0.01 or 0.1% glucose, and the culture media were replaced with fresh media every day to maintain the glucose concentrations. After 5 days, the bacteria were harvested, and the total lipids were extracted. The methanol-insoluble fraction was then obtained from 100 μg of each total lipid preparation and analyzed by TLC. *B*, GMM-specific, CD1b-restricted TCR-expressing Jurkat T cells were cocultured with either C1R/CD1b or C1R/mock in the presence of different concentrations of the total lipids derived from the 0.1% glucose-containing (*upper panel*) and the 0.01% glucose-containing (*lower panel*) cultures. The T cell response was assessed by measuring IL-2 released into the media.

GMM Production Occurs in Mycobacteria-infected Tissues—A previous study detected GMM comigrating lipids can be derived from *Mycobacterium leprae*, raising the possibility that GMM is produced by mycobacteria in tissues (5). However, the chemical structures of such candidate glycosyl mycolates could not be directly determined, and it remained unknown whether *M. tuberculosis* produces GMM during infection. Therefore, we infected CH3 mice with *M. tuberculosis* Erdman strain and isolated mycobacteria directly from the lungs after ~3 weeks of infection. Bacteria were enriched from lung preparations by centrifugation and treatment with weak base to disperse lung tissue. The resulting preparations contained predominantly mycobacterial lipids when analyzed by LC-MS (data not shown). By comparing total *M. tuberculosis* lipids from lung with an *M. fallax* GMM standard in LC-MS experiments, we analyzed the *in vivo* derived lipids that nearly copurified with the GMM standard. Mass measurements with an Accurate Mass QTOF capable of mass resolution of 10 ppm detected an ion at 1317.2577 in lung-derived lipids (Fig. 6*A*). Both the absolute *m/z* and the isotope ratios matched the predicted masses of an ammonium adduct of a GMM carrying a C_{78} α-mycolic acid within expected error (C_{84}, $H_{162}O_8$, C_{78} GMM, expected *m/z* 1317.2613). Further supporting the identification of this ion as GMM, mycolic acid derivatives are characteristically synthe-

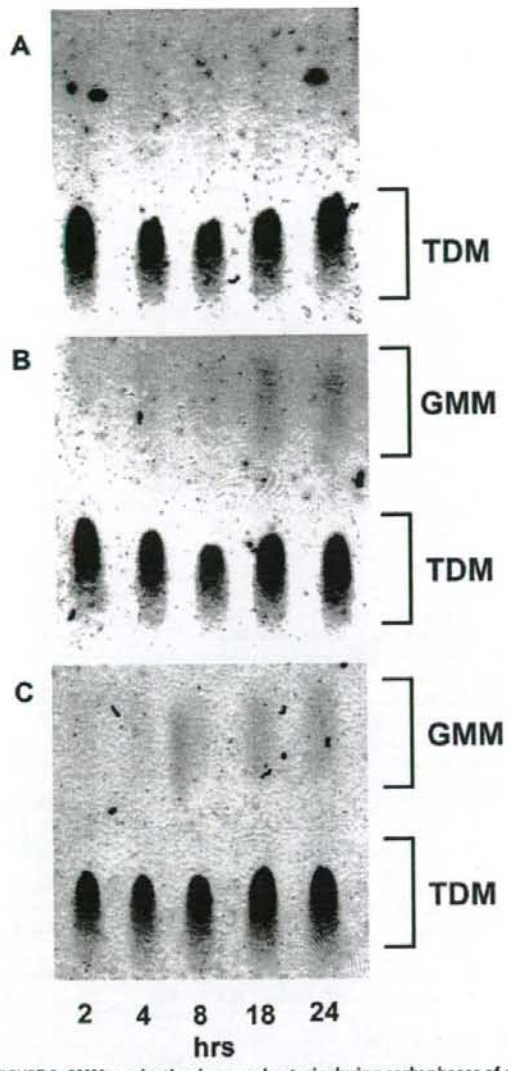

FIGURE 5. **GMM production by mycobacteria during early phases of culture.** MAC was cultured either in liquid media containing 0.01% (*A*) or 0.1% (*B*) glucose or in human serum (*C*). At indicated time points, the bacteria were harvested, and the total lipids were analyzed by TLC.

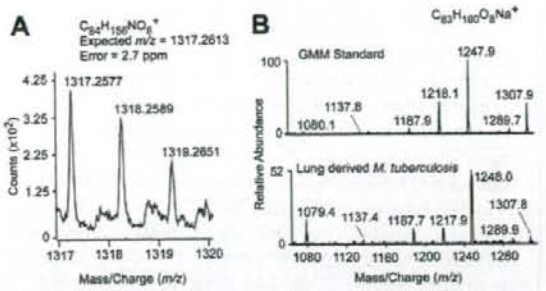

FIGURE 6. **GMM production *in vivo* by *M. tuberculosis*.** *A*, among the mixture of lipids extracted from *M. tuberculosis* derived from mouse lungs, lipids that copurified with a GMM standard were analyzed in the positive mode on an Accurate Mass QTOF MS. The detected mass of *m/z* 1317.2577 corresponds to the predicted mass of an ammonium adduct of C_{78} GMM (*m/z* 1317.2613). *B*, positive mode CID-MS analysis in ion trapping mass spectrometry of *M. fallax* GMM and the lung-derived candidate GMM molecule detected as sodium adducts show a similar pattern of product ions.

sized as a series of molecules that differ from one another by mass increments corresponding to C_2H_2, and the spectrum of the lung-derived lipids contained two additional ions (*m/z* 1345.3033, 1289.2304) corresponding to the expected masses of C_{80} and C_{76} GMM (data not shown). Finally, a separate CID-MS experiment, carried out with an *M. fallax* GMM standard and the lung-derived lipids, showed nearly identical product ions, including ions with mass intervals corresponding to the loss of 60, 90, and 120 units (*m/z* 1248.0, 1217.9, and 1187.7), which likely represent the loss of $C_2H_4O_2$, $C_3H_6O_3$, and $C_4H_8O_4$, which are products expected from cleavage through the hexose sugar (Fig. 6*B*). These data provide strong evidence that GMM is made in the host *in vivo* during an experimental infection.

DISCUSSION

MAC represents a group of environmental mycobacteria that have evolved the capacity to adapt to low nutrition environments. In fact, MAC can survive and replicate in water supply systems (1), where aggregates of the microbes exist in close association with the surface area. This biofilm formation confers significant resistance to a variety of physical and chemical stresses, such as exposure to disinfectants and antibiotics, and thus is an important strategy for the environmental mycobacteria to maintain their life cycles safely in natural environments. These environmental mycobacteria stably express TDM on the surface of their cell wall but fail to biosynthesize GMM because of highly limited availability of glucose. This study argues that, upon entry into the host, this glycolipid phenotype would be modified enzymatically by utilizing the host-derived glucose as a substrate. All three functional mycolyltransferases (Ag85A, Ag85B, and Ag85C) identified in *M. tuberculosis* (18) appear capable of catalyzing TDM synthesis from TMM *in vitro*, and the corresponding Ag85 isoforms have been found also in *M. avium*. Although these enzymes have certain overlapping functions, their differential transcription patterns have been noted in mycobacteria grown under distinct conditions. Ag85A is an isoform that is preferentially expressed in macrophage-resident mycobacteria (19, 20), and thus, its catalytic potential for the TDM-GMM exchange could have an impact on macrophage functions if TDM and GMM have differential ability to activate the cells. Indeed, we recently found that interferon-γ-primed macrophages produced only a marginal level of nitric oxides when stimulated with GMM, which contrasted sharply with those stimulated with TDM that were capable of mounting robust nitric oxide responses (data not shown). Therefore, the TDM-GMM exchange may be valuable in minimizing the nitric oxide response by the host macrophages. Prior to this report, the identity of any mycolyltrans-

ferase that could produce GMM was unknown, so these results establish that Ag85A has this function.

Once pathogens break the frontline defense mediated by the host innate immunity, they are then challenged by specific T lymphocytes that belong to the acquired immunity. Glycolipid-specific T lymphocyte reactions are elicited in humans and guinea pigs infected with mycobacteria, and activation of these T cells is restricted not by the classical major histocompatibility complex-encoded class I and class II molecules but rather by nonmajor histocompatibility complex-encoded group 1 CD1 molecules (CD1a, CD1b, and CD1c in humans) (21). These CD1 molecules are expressed in activated macrophages as well as dendritic cells, the two major cell types for mycobacterial infection. Notably, infiltration of GMM-specific, CD1b-restricted T cells is detected in human skin infected with *M. leprae*, and the human T cell lines (7) and polyclonal T cells (22) exhibit cytotoxic effects, suggesting that the CD1-restricted T cell response directed against GMM could potentially function to clear infection. Taken together, these results raise an interesting possibility that GMM generated as a result of TDM-GMM exchange functions to reduce the innate immune response, but provides the host with a new opportunity to monitor live mycobacteria and eliminate them in the subsequent phases of the acquired immunity. This may represent an example of how the immune system has been constructed during the long processes of evolution to fight efficiently against pathogens.

Despite the fact that GMM is produced by pathogenic mycobacteria and structurally related to the well studied TDM, it has not been the target for focused investigation until recently. Presumably, this is partly because only a tiny amount of GMM, as compared with TDM, is synthesized by pathogenic slow growing mycobacteria, such as *M. tuberculosis* and *M. avium*, when cultured in the Middlebrook "standard" media formulations. Ironically, the standard media used for cultivation of fast growing saprophytic bacteria, such as *Rhodococcus ruber*, contain 1% glucose, and thus, the nonpathogenic bacteria cultured in such a medium produce GMM abundantly, and its structure and biological activities have been studied extensively (6, 23). In many previous studies, the composition, structure, and function of mycobacterial lipids were determined by using bacteria grown in standard media, but the present study suggests that the "lipid world" that is constructed by the bacteria grown in standard culture conditions is substantially different from the lipid world constructed as a result of interaction with the continuously changing host environments.

Acknowledgments—We thank Dr. Seiko Mizuno (Soai University, Osaka, Japan) for use of the GC-MS facility and Dr. Tan-Yun Cheng (Brigham and Women's Hospital, Harvard Medical School, Boston, MA) for reagents and advice.

REFERENCES

1. Primm, T. P., Lucero, C. A., and Falkinham, J. O., III (2004) *Clin. Microbiol. Rev.* **17,** 98–106
2. Sathyamoorthy, N., and Takayama, K. (1987) *J. Biol. Chem.* **262,** 13417–13423
3. Ryll, R., Kumazawa, Y., and Yano, I. (2001) *Microbiol. Immunol.* **45,** 801–811
4. Brennan, P., and Ballou, C. E. (1967) *J. Biol. Chem.* **242,** 3046–3056
5. Moody, D. B., Guy, M. R., Grant, E., Cheng, T. Y., Brenner, M. B., Besra, G. S., and Porcelli, S. A. (2000) *J. Exp. Med.* **192,** 965–976
6. Matsunaga, I., Oka, S., Inoue, T., and Yano, I. (1990) *FEMS Microbiol. Lett.* **55,** 49–53
7. Moody, D. B., Reinhold, B. B., Guy, M. R., Beckman, E. M., Frederique, D. E., Furlong, S. T., Ye, S., Reinhold, V. N., Sieling, P. A., Modlin, R. L., Besra, G. S., and Porcelli, S. A. (1997) *Science* **278,** 283–286
8. Matsunaga, I., Bhatt, A., Young, D. C., Cheng, T. Y., Eyles, S. J., Besra, G. S., Briken, V., Porcelli, S. A., Costello, C. E., Jacobs, W. R., Jr., and Moody, D. B. (2004) *J. Exp. Med.* **200,** 1559–1569
9. Enomoto, Y., Sugita, M., Matsunaga, I., Naka, T., Sato, A., Kawashima, T., Shimizu, K., Takahashi, H., Norose, Y., and Yano, I. (2005) *Biochem. Biophys. Res. Commun.* **337,** 452–456
10. Kremer, L., Maughan, W. N., Wilson, R. A., Dover, L. G., and Besra, G. S. (2002) *Lett. Appl. Microbiol.* **34,** 233–237
11. Cheng, T. Y., Relloso, M., Van Rhijn, I., Young, D. C., Besra, G. S., Briken, V., Zajonc, D. M., Wilson, I. A., Porcelli, S., and Moody, D. B. (2006) *EMBO J.* **25,** 2989–2999
12. Grant, E. P., Degano, M., Rosat, J. P., Stenger, S., Modlin, R. L., Wilson, I. A., Porcelli, S. A., and Brenner, M. B. (1999) *J. Exp. Med.* **189,** 195–205
13. Sugita, M., Porcelli, S. A., and Brenner, M. B. (1997) *J. Immunol.* **159,** 2358–2365
14. Barry, C. E., III, Lee, R. E., Mdluli, K., Sampson, A. E., Schroeder, B. G., Slayden, R. A., and Yuan, Y. (1998) *Prog. Lipid. Res.* **37,** 143–179
15. Natsuhara, Y., Oka, S., Kaneda, K., Kato, Y., and Yano, I. (1990) *Cancer Immunol. Immunother.* **31,** 99–106
16. Anderson, D. H., Harth, G., Horwitz, M. A., and Eisenberg, D. (2001) *J. Mol. Biol.* **307,** 671–681
17. Ohara, N., Matsuo, K., Yamaguchi, R., Yamazaki, A., Tasaka, H., and Yamada, T. (1993) *Infect. Immun.* **61,** 1173–1179
18. Belisle, J. T., Vissa, V. D., Sievert, T., Takayama, K., Brennan, P. J., and Besra, G. S. (1997) *Science* **276,** 1420–1422
19. Hou, J. Y., Graham, J. E., and Clark-Curtiss, J. E. (2002) *Infect. Immun.* **70,** 3714–3726
20. Mariani, F., Cappelli, G., Riccardi, G., and Colizzi, V. (2000) *Gene (Amst.)* **253,** 281–291
21. Matsunaga, I., and Sugita, M. (2007) *Curr. Immunol. Rev.* **3,** 145–150
22. Ulrichs, T., Moody, D. B., Grant, E., Kaufmann, S. H., and Porcelli, S. A. (2003) *Infect. Immun.* **71,** 3076–3087
23. Matsunaga, I., Oka, S., Fujiwara, N., and Yano, I. (1996) *J. Biochem. (Tokyo)* **120,** 663–670

International Immunology, Vol. 20, No. 9, pp. 1169–1180
doi:10.1093/intimm/dxn074

Soluble G protein of respiratory syncytial virus inhibits Toll-like receptor 3/4-mediated IFN-beta induction

Masashi Shingai[1,4], Masahiro Azuma[1], Takashi Ebihara[1], Miwa Sasai[1,5], Kenji Funami[1,6], Minoru Ayata[2], Hisashi Ogura[2], Hiroyuki Tsutsumi[3], Misako Matsumoto[1] and **Tsukasa Seya[1]**

[1]Department of Microbiology and Immunology, Hokkaido University Graduate School of Medicine, Kita-15, Nishi-7, Kita-ku, Sapporo 060-8638, Japan
[2]Department of Virology, Osaka City University, Asahimachi 1-4-3, Abeno-ku, Osaka 545-8585, Japan
[3]Department of Pediatrics, Sapporo Medical University, School of Medicine, Minami-1, Nishi-16, Chuoh-ku, Sapporo 060-8543, Japan

[4]Present address: Laboratory of Molecular Microbiology, National Institute of Allergy and Infectious Diseases, National Institutes of Health, Bethesda, MD 20892, USA
[5]Present address: Section of Immunobiology, Yale University School of Medicine, 300 Cedar Street, TAC S640, New Haven, CT 06520, USA
[6]Present address: Medical Research Center, Keio University, Shinanomachi 35, Shinjuku-ku, Tokyo 160-8582, Japan

Keywords: dendritic cells, respiratory syncytial virus, TICAM-1 (TRIF), Toll-like receptor, type I IFNs

Abstract

Monocyte-derived dendritic cells (mDCs) recognize viral RNA extrinsically by Toll-like receptor (TLR) 3 on the membrane and intrinsically retinoic acid-inducible gene I (RIG-I)/melanoma differentiation-associated gene 5 (MDA5) in the cytoplasm to induce type I IFNs and mDC maturation. When mDCs were treated with live or UV-irradiated respiratory syncytial virus (RSV), early (~4 h) induction of IFN-β usually occurs in other virus infections was barely observed. Live RSV subsequently replicated to activate the cytoplasmic IFN-inducing pathway leading to robust type I IFN induction. We found that RSV initial attachment to cells blocked polyI:C-mediated IFN-β induction, and this early IFN-β-modulating event was abrogated by antibodies against envelope proteins of RSV, demonstrating the presence of a IFN-regulatory mode by early RSV attachment to host cells. By IFN-stimulated response element (ISRE) reporter analysis in HEK293 cells, polyI:C- or LPS-mediated ISRE activation was dose dependently inhibited by live and inactive RSV to a similar extent. Of the RSV envelope proteins, simultaneously expressed or exogenously added RSV G or soluble G (sG) proteins inhibited TLR3/4-mediated ISRE activation in HEK293 cells. sG proteins expressed in cells did not affect the RIG-I/MDA5 pathway but inhibited the TLR adaptor TRIF/TICAM-1 pathway for ISRE activation. Finally, extrinsically added sG protein suppressed the production of IFN-β in mDCs. Although the molecular mechanism of this extrinsic functional mode of the RSV G glycoprotein (G protein) remains undetermined, G proteins may neutralize the fusion glycoprotein function that promotes IFN-mediated mDC modulation via TLR4 and may cause insufficient raising cell-mediated immunity against RSV.

Introduction

Respiratory syncytial virus (RSV) is a member of the Paramyxoviridae family consisting of a negative-strand RNA genome in a nucleocapsid. RSV preferentially infects airway epithelial cells, causing bronchiolitis and respiratory infections (1) and can exacerbate asthma and chronic obstructive pulmonary diseases (1). However, an effective vaccine for RSV is not yet available. Recurrent RSV infections are often observed in humans, and this is due to the failure of the hosts to raise long-lasting immunity against RSV (1). Recent reports suggested that cell-mediated immunity, including CTLs, NK and B cells, develops followed by maturation of monocyte-derived dendritic cells (mDCs) (2). These

Correspondence to: T. Seya; E-mail: seya-tu@pop.med.hokudai.ac.jp
Transmitting editor: T. Takai

Received 20 September 2007, *accepted* 9 June 2008
Advance Access publication 8 July 2008

lymphocytes produce IFN-γ which orchestrates the acquired immune response to eradicate viral infection (3). Toll-like receptors (TLRs), retinoic acid-inducible gene I (RIG-I)-like receptors and NOD-like receptors are expressed in dendritic cells (DCs) and play a major role in driving the lymphocyte-mediated immune responses (4). Possible involvement of TLR3 and its response in RSV infectious signs has been reported (5–7), although how RSV induces host immune modulation via the TLR3 remains largely unclear.

Type I IFNs serve as antiviral factors. Several reports have suggested the involvement of TLR3 (5, 7) and RIG-I (6) in RSV-mediated IFN-α/β induction and cellular responses. RIG-I preferentially recognizes 5′-triphosphate RNA (8, 9) in addition to double-stranded (ds)RNA, whereas TLR3 captures only dsRNA. Their signaling pathways partially overlap in that they converge upon the IFN-regulatory factor (IRF)-3-activating kinase complex for activation of the IFN-β promoter (10). Bronchial epithelial cells and mDCs preserve these receptors and downstream signaling pathways. mDC TLR3 particularly plays a crucial role in driving mDCs to direct CTL- and NK-inducing maturation as well as RSV infection-mediated type I IFN production (11, 12).

For induction of type I IFNs and NK/CTL activation, the cytoplasmic Toll–IL-1R (TIR) homology domain of TLR3 recruits the adaptor molecule TICAM-1 (TRIF) (13, 14), while LPS allows TLR4 to recruit the adaptor molecules TICAM-2 (TRAM) and TICAM-1 (15, 16). Thus, TICAM-1 is the common adaptor in the pathways of TLR3 and TLR4. Both pathways activate IRF-3 and IRF-7 through a MyD88-independent pathway, resulting in IFN-β production. Extrinsic supplement of viral dsRNA can activate the TICAM-1 pathway (17). On the other hand, RIG-I and melanoma differentiation-associated gene 5 (MDA5) reside in the cytoplasm and interact with a mitochondrial protein, IFN-β promoter stimulator 1 (IPS-1)/mitochondria antiviral signaling (MAVS)/VISA/Cardif, to activate IRF-3 and IRF-7 (18–21). Only intrinsically produced viral RNA is a ligand for the cytoplasmic IFN-inducing sensors. Studies on how these pathways evoke mDC-mediated cellular immunity are in progress with special interest (22). Although there is a MyD88-dependent pathway for IFN induction in plasmacytoid DCs (23–25), this pathway does not function in mDCs. Accordingly, we focus on the role of the TICAM-1 and IPS-1 pathways in RSV-mediated mDC functional modulation.

In the virus side, what RSV factors are associated with modulation of mDC maturation remain largely unknown. In cytoplasmic RSV proteins, the NS1 and NS2 proteins are shown to antagonize IFN response (26, 27). Nevertheless, type I IFN is induced in RSV-replicating cells although the amounts of IFN are relatively low. The envelope of RSV contains three transmembrane surface proteins, the fusion glycoprotein (F protein), G glycoprotein (G protein) and SH protein. F protein is responsible for fusion of the viral envelope with the plasma membrane of the host target cell (28). The F protein may induce activation of nuclear factor-κB (NF-κB) and the IFN-β promoter via TLR4 (29, 30). In addition, the F protein of RSV serves as an agonist of TLR4 and induces pro-inflammatory cytokines (29). On the other hand, the G protein, which mediates attachment of the virus particle to the target cell (31), and SH protein are not functionally well understood (32). Infected cells also produce a smaller secreted form of the G protein [soluble G (sG) protein] besides the transmembrane type G protein (33). The RSV G protein has been implicated in altered cytokine and chemokine expression by pulmonary leukocytes (34). Yet, there has been no report on the RSV surface proteins that affect cytoplasmic IFN-inducing events. Accordingly, no report has mentioned the possible association between the RSV G/SH proteins and the TLR pathways in RSV infection.

Here, we discovered a role of the RSV G protein in mDC IFN response. This protein inhibits the TLR3/4-mediated IFN-β promoter activation through RSV–host cell interaction. A possible target for the G protein attachment to cells is the TICAM-1 pathway, thereby TLR3/4-mediated type I IFN induction being prohibited. The RSV G protein may act as a buffer for evoking cell-mediated TLR3/4-derived immunity. Possible roles for the function of the G protein in the RSV infection are also discussed.

Methods

Cell culture, viruses and reagents

HEp-2, Vero and HEK293 cells were maintained in DMEM (Invitrogen, San Diego, CA, USA) supplemented with 10% heat-inactivated FCS (JRH Biosciences, Lenexa, KS, USA) and antibiotics. Human RSV field-isolate strain (RSV2177) in subgroup B was isolated and propagated with HEp-2 cells. The accession numbers of *NS1*, *NS2*, *N*, *G*, *F* and *SH* genes were AB245473–AB245478. The titer of RSV2177 was determined by 50% tissue culture infective dose with HEp-2 cells. Measles virus (MV) Edmonston strain was passaged and titrated in Vero cells. RSV and MV were inactivated by UV irradiation at 1.5 J cm^{-2}. Poly I:C was purchased from Amersham Pharmacia Biotech (Buckinghamshire, UK). Polymyxin B, LPS from *Escherichia coli* serotype 0111:B4, was from Sigma Chemical Co., St Louis, MO, USA. The mycoplasma lipopeptide macrophage-activating lipopeptide-2 (MALP-2) was prepared as described (35). MALP-2 and poly I:C were treated with polymyxin B (10 μg ml^{-1}) (an LPS inhibitor) for 1 h at 37°C before stimulation of cells (35). Usually, 50 or 10 μg ml^{-1} of poly I:C, 100 ng ml^{-1} of LPS and 100 nM of MALP-2 were utilized for TLR stimulation. Mouse IgG, mouse IgG2b and anti-Flag M2 mAb and anti-Flag polyclonal antibodies were obtained from Sigma; anti-CD80 and anti-HLA-DR mAbs were obtained from Immunotech (Marseille, France); anti-CD83 mAb was obtained from Cosmo Bio (Tokyo, Japan); anti-CD86 mAb was obtained from Ancell (Bayport, MN, USA); anti-CD40 mAb was from PharMingen (San Diego, CA, USA); FITC-conjugated goat anti-mouse and anti-rabbit IgG $F(ab')_2$ and HRP-conjugated goat anti-rabbit Igs were obtained from American Qualex Manufacturers (Bayport San Clemente, CA, USA) and FITC-labeled and non-labeled goat anti-RSV polyclonal antibody was from Chemicon.

Preparation of DCs (mDCs)

Human PBMCs were isolated from buffy coat of normal healthy donors by methylcellulose sedimentation followed by standard density-gradient centrifugation with Ficoll–Hypaque (Amersham Biosciences, Piscataway, NJ, USA) (35). For human immature DC preparation, CD14-positive monocytes

were prepared from huPBMC by using MACS system (Miltenyi Biotec, Gladbach, Germany) with anti-human CD14 mAb-conjugated microbeads and kept in RPMI-1640 (Invitrogen) containing 10% FCS, 500 IU ml^{-1} human granulocyte macrophage colony-stimulating factor, 100 IU ml^{-1} human IL-4 (Pepro Tech, London, UK) and antibiotics for 6 days. Morphological changes were examined by phase contrast microscopy (Olympus IX-70, Tokyo, Japan).

FACS cytometric analysis of cell-surface antigens

FACS methods were described previously (35). Briefly, cells were suspended in PBS containing 0.1% sodium azide and 1% BSA (FACS buffer) and incubated for 30 min at 4°C with relevant or control mAbs, followed by FITC-labeled anti-mouse IgG $F(ab')_2$. In some experiments, cells were directly stained with FITC-labeled anti-RSV polyclonal antibody. Cells were washed, and their fluorescence intensities were measured by FACS.

Determination of human tumor necrosis factor-α and IFN-β level

Quantitative PCR and ELISA were used for this purpose. Culture media were centrifuged to remove cell debris and the supernatants were stored at −80°C until the assay. The level of secreted human tumor necrosis factor-α (TNF-α) or IFN-β in the culture medium was determined with ELISA kits (Amersham Pharmacia and FUJIREBIO, Tokyo, Japan). The detection limits of human TNF-α and IFN-β were <5 pg ml^{-1} and <2.5 U ml^{-1}, respectively. Quantitative PCR and the primers for this assay were performed as described previously (36).

RSV sequences and plasmid construction

Total RNA from RSV2177-infected HEp-2 cells was extracted with RNeasy mini kit (Qiagen). After DNase treating, 1 μg of total RNA was incubated at 70°C for 5 min, kept on ice for 2 min and reverse transcription was performed with MMLV–reverse transcriptase (Promega, Madison, WI, USA) at 37°C for 90 min followed by PCR. Detection of RSV subgroup was performed by PCR with subgroup-specific primer sets (37) (RSV/SH A 5′-TCGAGTCAACACATAGCATTC-3′ and RSV/F1 5′-CAACTCCATTGTTATTTGCC-3′ for RSV subgroup A and RSV/SH B 5′-CATAGTATTCTACCATTATGC-3′ and RSV/F1 for RSV subgroup B). Direct sequences were detected from the amplified PCR fragments with conserved sequence primer sets among RSVs (RSV/Fm01 5′-GGCAAATAACAATGGAGYTGC-3′ and RSV/Fg01 5′-TTGTWRRAACATGATYAGGTG-3′ for F gené, RSV/Gm01 5′-GGCAAATGCAACCATGTCCAA-3′ and RSV/Gg01 5′-ACCCAATCACATGCTTAGTTATTC-3′ for G gene, RSV/SHm01 5′-ATGGGAAATACATCCAT-3′ and RSV/SHg01 5′-CACAGCATAATGGTAGA-3′ for SH gene and RSV/NPm01 5′-ATGGCTCTTAGCAAAG-3′ and RSV/NPg01 5′-TTAAAGCTCTACATCAT-3′ for NP gene). The nucleotide sequences of these PCR fragments were confirmed by direct sequencing. The consensus sequences obtained from the amplicons were inserted into a plasmid vector (pEFBos or $pCXN_2$), and the clones were modified by addition of Flag-tag, exchanging of signal sequence and/or truncation of the cytoplasmic and transmembrane regions.

Plasmid transfection and luciferase assay

A luciferase reporter plasmid, pISRE-Luc, was from Stratagene (Stratagene, La Jolla, CA, USA) and pELAM-Luc reporter plasmid was constructed as referred in Kurt-Jones *et al.* (29). pRL-TK vector was from Promega. A plasmid for human TLR3 and TICAM-1 expression was described previously (13). Plasmids for human TLR4, MD-2 and CD14 expression were kindly provided by K. Miyake (The University of Tokyo, Tokyo), TANK-binding kinase 1 (TBK1) expression by M. Nakanishi (The Nagoya City University, Nagoya) and IκB kinase-related kinase ε (IKKε) expression by T. Maniatis (Harvard Medical School, Boston, MA, USA). Plasmids for constitutive active forms of RIG-I and MDA5 (ΔRIG-I and MDA5N) expression were kindly provided by T. Fujita (The University of Kyoto, Kyoto). All transfection was carried out on HEK293 cells growing on 24-well plates. Usually, 100 ng of TLR3/pEFBos or TLR4/pEFBos, 100 ng of MD-2/pEFBos, 100 ng of CD14/pEFBos, 100 ng of luciferase reporter gene plasmid (firefly luciferase, experimental reporter) and 3 ng of pRL-TK vector (Renilla luciferase for internal control) were introduced into cells by LipofectAMINE 2000 (Invitrogen) according to the manufacture's procedure. At 24 h post-transfection, cells were stimulated with various stimulators for 6 h. Cells were then harvested with trypsin, washed with PBS and treated with 20 μl of Passive Lysis Buffer (Promega). After 6-h incubation, cells were lysed with lysis buffer and the assay was performed using dual-luciferase reporter assay system. Fold induction against the control medium is indicated.

Immunoprecipitation, SDS–PAGE and western blotting

Cells were washed in PBS (pH 7.4) and solubilized with 100 μl of 1% (v/v) Triton X-100 containing 137 mM NaCl, 2 mM EDTA and 1 mM phenylmethylsulfonylfluoride. After centrifugation (10 000 × *g* for 10 min), proteins in cell lysate or culture supernatant were immunoprecipitated with anti-Flag mAb. Immunoprecipitants were washed and eluted with Flag peptide. The eluted samples were heated or non-heated and were subjected to SDS–PAGE under reducing or non-reducing conditions. Proteins were transferred onto nylon membranes. The membranes were incubated with 10% skimmed milk containing 5% goat serum for 30 min at room temperature, followed by the addition of anti-Flag pAbs. One hour later, the membranes were washed extensively with PBS containing 0.5% Tween 20 and then incubated with 5 μg of HRP-conjugated goat anti-rabbit IgG antibody for 1 h at 37°C. Following second incubation, the membranes were washed with PBS–Tween 20 and proteins were detected with an ECL chemiluminescence kit (Amersham Biosciences).

Endoglycosidase digestion

Protein samples were made up to a final concentration of either 100 mM Tris–HCl (pH 8.6), 0.1% SDS and 1% NP-40 or 50 mM sodium citrate (pH 5.0) and 0.5% SDS and incubated at 37°C for 14 h with endoglycosidase F (Takara) or endoglycosidase H (Seikagaku Corporation, Tokyo, Japan), respectively, as previously reported (38). The samples were analyzed on SDS–PAGE under reducing and non-reducing conditions.

RSV treatment of human cells

Human cells (mDCs and HEK293 cells) were transfected with pGV-E2/huELAM (ELAM promoter-linked firefly luciferase) or pISRE-Luc [IFN-stimulated response element (ISRE) promoter-linked firefly luciferase] and phRL-TK (thymidin kinase with Renilla luciferase). The last one is the internal control. Twenty-four hours later, cells were washed and treated with live or UV-irradiated RSV [multiplicity of infection (MOI) = 0.5, otherwise indicated], LPS or medium. In some experiments, antibodies against RSV proteins (20 μg ml^{-1}) were added to the cells together with UV-irradiated RSV (MOI = 1.0). The cells were lysed with lysis buffer at the indicated time points and the assay was performed using dual-luciferase reporter assay system. Fold induction against the control medium is indicated at each time point.

Inhibitory effect of the sG protein on the ISRE promoter was tested as follows. The supernatant containing the secreted G protein, UV-irradiated RSV, UV-irradiated MV or medium were added to HEK293 cells, and then cells were transfected with TICAM-1/pEFBos (50 ng), IKKε/pcDNA3.1 (200 ng), TBK1/pcDNA3.1 (200 ng), MAVS/pEFBos (400 ng), ΔRIG-I/pEFBos (700 ng) or MDA5N/pEFBos or pEFBos (700 ng) and 100 ng of pISRE and 3 ng of pRL-TK. Six hours later, cells were harvested with trypsin, washed with PBS and treated with 20 μl of Passive Lysis Buffer. Luciferase activities were measured by Dual-Luciferase assay kit (Promega). The luciferase activity of firefly was normalized by that of Renilla and relative fold activation to the medium control was determined. All experiments were performed in triplicate.

Results

Immune responses induced in human DCs by RSV stimulation

DCs in the respiratory tract play important roles in the immune response against RSV infection. Human mDCs prepared from three healthy donors were incubated with RSV at MOI = 0.5. Viral proteins were detected on the mDC surface within 24 h and kept expressed over 48 h using anti-RSV polyclonal antibodies by FACS analysis (Fig. 1A). Thus, human mDCs are susceptible to RSV of this subgroup B isolate.

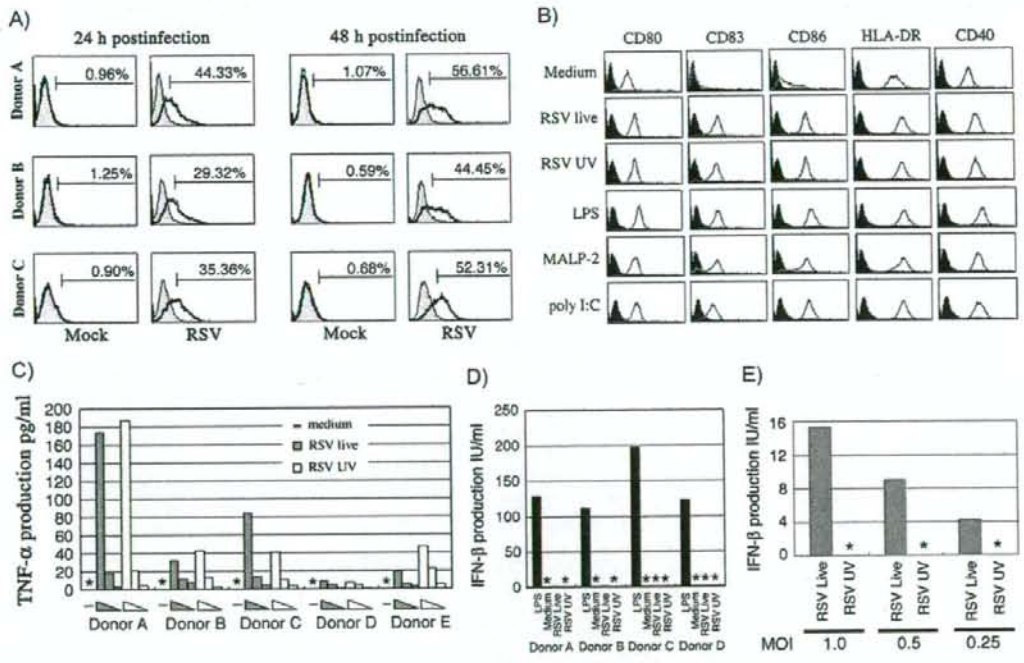

Fig. 1. Human DCs responding to RSV. (Panel A) Human immature mDCs are susceptible to RSV infection. Immature mDCs were incubated with Mock or RSV (MOI = 0.5). These mDCs were stained with FITC-labeled goat anti-RSV polyclonal antibodies or FITC-labeled control mouse Ig 24 or 48 h after RSV infection. %RSV-positive cells are indicated in the FACS histograms. (Panel B) mDC maturation is induced by RSV treatment. Immature mDCs were treated with indicated TLR ligands, medium only or RSV (live or UV irradiated, MOI = 0.5). Twenty-four hours later, mDCs were allowed to react with the indicated antibodies of $F(ab')_2$ against mDC maturation markers (open histograms). Isotype-matched IgG was used as controls (closed histograms). The experiments were performed three times and represented results are shown. (Panel C) Production of TNF-α by mDCs treated with live or UV-irradiated RSV. Human immature mDCs were prepared from five healthy donors and individually treated with RSV (live or UV irradiated) at MOI = 0.5, 0.25 and 0.1. The culture supernatants of the mDCs were harvested in 24 h and the levels of TNF-α determined by ELISA. Asterisk means 'not detected'. (Panels D and E) Production of IFN-β by mDCs in response to RSV. Immature mDCs were treated with RSV (live or UV irradiated) at MOI = 0.5 (otherwise indicated). LPS (100 ng ml^{-1}) or medium were used as controls. Twenty-four hours later, the supernatants were collected, and the levels of IFN-β were measured by ELISA. Asterisk, not detected.

To examine DC maturation by RSV, mDCs were stimulated with live or UV-irradiated RSV, LPS (TLR4 ligand), MALP-2 (TLR2 ligand) or polyI:C (TLR3 ligand) (Fig. 1B). Stimulation with either live or UV-irradiated RSV led to maturation of mDC as determined by cell-surface markers (CD80, CD83, CD86, HLA-DR and CD40) as was the case with the other TLR ligands. Since UV-irradiated RSV induced mDC maturation, RNA replication after viral entry is not a main cause for the RSV-mediated mDC maturation.

Next, we examined if mDCs produce TNF-α and IFN-β in response to RSV infection/stimulation. TNF-α is induced mainly through NF-κB activation and known to mature mDCs. mDCs from various individuals were incubated with the indicated doses of live or UV-irradiated RSV (Fig. 1C). LPS was used as a positive control for the TLR4 ligand. Twenty-four hours later, the supernatants were collected for ELISA. The levels of TNF-α were increased in the supernatant of mDCs in a RSV dose-dependent manner irrespective of RSV treatment, live or UV irradiation (Fig. 1C). Thus, viral attachment to cells rather than replication triggers TNF-α production. However, IFN-β was barely produced in mDCs treated with RSV (Fig. 1D). Although higher doses of live RSV minimally induce IFN-β (<20 IU ml^{-1}) in mDCs during 24 h (i.e. replication dependently, presumably via the cytoplasmic pathway), UV-irradiated RSV did not induce IFN-β by MOI = 1.0 (Fig. 1E) and even at MOI = 5 (data not shown). Although IFN-β induction appears to occur by stimulation of TLR4 with the F protein (30), this is not the case in challenge with UV-irradiated RSV. mDC maturation with TNF-α production but poor IFN-β production is a characteristic phenotype in RSV-affected human mDCs.

Quantitative PCR analysis was performed with mDCs for surveying cytokine induction. UV-inactivated RSV induced a minute amount of the IFN-β message in mDCs but failed to induce it >6 h after stimulation, although live RSV allowed mDCs to induce incremental IFN-β >12 h post-infection (p.i.) (Fig. 2A). In contrast, the TNF-α was somehow kept to be constant >12 h in inactive RSV-stimulated mDCs (Fig. 2B). We consistently found that IFN-inducible genes were barely up-regulated by function of UV-irradiated RSV even after 6 h (data not shown) and 24 h post-stimulation (Fig. 2C). IFN-inducible genes were up-regulated only when mDCs were challenged with high doses of live RSV after 12 h. According to the ~4 h mRNA levels and 24 h ELISA results, RSV-mediated robust IFN induction is the replication-dependent event.

RSV inhibits virus–cell contact-mediated IFN-β induction

UV-inactivated RSV induced TNF-α but barely induced IFN-β in the early phase of mDCs. We asked what causes the impotent production of IFN-β in response to the external stimulation of RSV. We tested the reporter-activating abilities of RSV using the ELAM (for NF-κB) and ISRE (for IFN-β) reporter assays in HEK293 cells. Neither of the promoters was activated in response to UV-irradiated RSV at the indicated time points (Fig. 3A and B). Live RSV on the other hand prominently activated ISRE by ~24 h p.i. (Fig. 3B) and ELAM >12 h p.i. (Fig. 3A). This activation was not due to contaminating LPS since the HEK293 cells did not express TLR4 (Fig. 3A and B). The RSV replication-dependent events will markedly happen >12 h p.i..

A previous report (29) demonstrated that the RSV F protein serves as a TLR4 agonist. Thus, virus–cell contact by live and UV-irradiated RSV should extrinsically activate NF-κB via the TLR4 pathway independent of viral replication. This issue was confirmed with HEK293 cells expressing TLR4 and the stimulation period by 6 h (Fig. 3C and D). ELAM promoter activation was observed in response to live and UV-inactive RSV to a similar extent (Fig. 3C). However, virtually no ISRE activation was detected under this setting (Fig. 3D). Hence, RSV activates the IFN-β promoter in an only replication-competent fashion >24 h p.i.. There is a discrepancy between NF-κB and IFN-β promoter activation.

When HEK293 cells expressing TLR4 were stimulated with LPS and various doses of live or UV-irradiated RSV, RSV dose dependently inhibited LPS-mediated activation of the ISRE promoter (Fig. 4A) irrespective of irradiation, since the analysis was performed within 12 h i.e. before significant viral replication. To test if the inhibition was RSV (but not TLR4) specific, TLR3-expressing HEK293 cells were stimulated with polyI:C in concert with various doses of live or UV-irradiated RSV. Both live and UV-irradiated RSV dose dependently inhibited ISRE promoter activation by polyI:C in terms of TLR3 signaling (Fig. 4B). We confirmed the suppression of IFN-β induction by RSV in mDCs. IFN-β protein production by LPS or polyI:C (determined 24 h p.i.) was also dose dependently inhibited by UV-irradiated RSV in mDCs (Fig. 4C). Function-neutralizing studies were performed using polyclonal antibodies against RSV envelope proteins. We set the conditions where polyI:C induced activation of the ISRE promoter in HEK cells and this activation was partly inhibited in response to live or UV-irradiated RSV that was administered for virus–cell contact (Fig. 4D). A typical result is shown in Fig. 4(D), where the pAb against RSV abrogated RSV-dependent inhibition of ISRE promoter activation. This implies that the virus–cell contact due to a RSV-exposing factor inhibits IFN-β promoter activation in host cells. Since the RSV F protein does not activate TLR3, we used the TLR3/polyI:C system in the following inhibition experiments.

RSV G protein is surface expressed to inhibit the IFN-β pathway

The question is what factor of the RSV envelope proteins participates in inhibition of polyI:C-derived IFN-β induction. Plasmid constructs were generated with the indicated RSV envelope proteins tagged with Flag (Fig. 5A). We confirmed protein expression in HEK293 cells using SDS–PAGE and western blotting with an anti-Flag antibody (Fig. 5B). Under reducing conditions, the F, G and sG proteins were detected on the blot at their expected molecular masses (Fig. 5B). Under non-reducing conditions, all these proteins tended to form multimers. In particular, the SH and F proteins formed multimers, which were partially dissociated upon heating and reduction (Fig. 5B), consistent with a previous report (28). The F, SH and G proteins, but not sG proteins, were N-glycosylated and no high mannose was detected on these

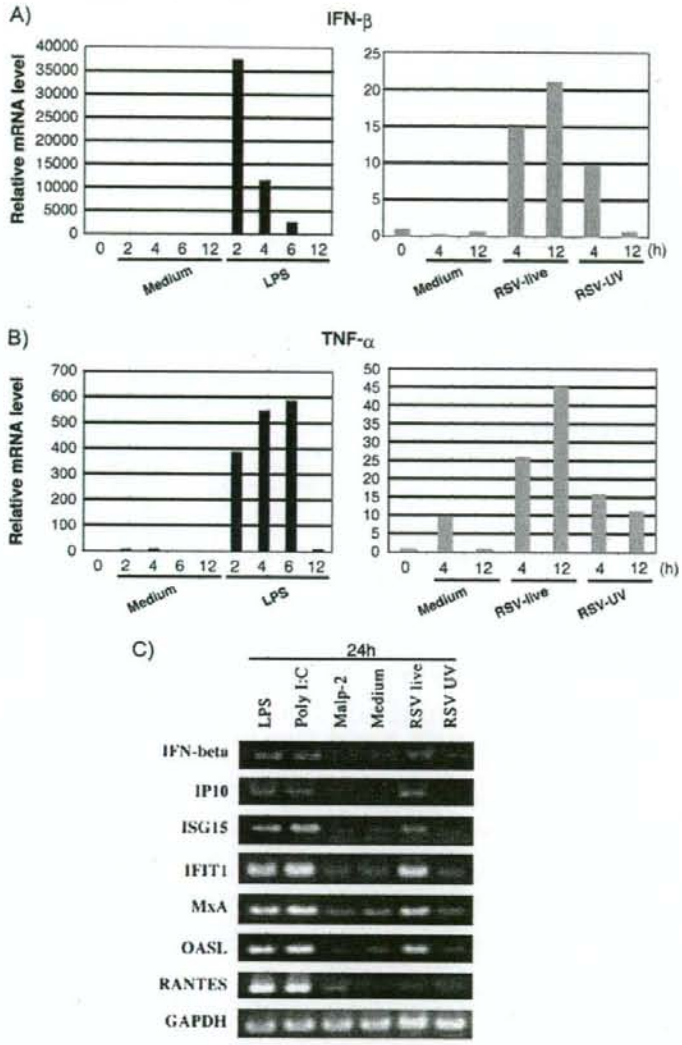

Fig. 2. Early induction of minute amounts of IFN-βthrough RSV–mDC interaction. (Panels A and B) Early induction of TNF-αand IFN-βby mDCs in response to RSV attachment. Human immature mDCs were treated with LPS (positive control), medium only (negative control) or live or UV-irradiated RSV (MOI = 0.5) as in Fig. 1(E). At indicated timed intervals, mRNA was harvested from the treated mDCs. Quantitative PCR was performed with these RNA samples pertaining to the cytokines indicated. (Panel C) Live RSV infects human mDCs and causes TLR3-independent induction of IFN-inducible genes. Human mDCs were stimulated with the reagents (indicated a top of the panel). The same lot of RSV (MOI = 0.5) as in Fig. 1(E)was used. Twenty-four hours later, mRNA levels of the indicated genes were assessed by reverse transcription–PCR. GAPDH is a control.

proteins (data not shown). Susceptibility of these proteins to glycosidases suggested that these proteins are expressed naturally on HEK293 cells. In addition, a soluble form of the G protein of 48 kDa with no high mannose or N-linked sugars was detected in the supernatant of the cells (Fig. 5C), consistent with a previous notion (33).

Cells were transfected with the indicated expression plasmid, together with TLR3-expressing plasmid and the reporter plasmids. Then, the cells were stimulated with polyI:C and after 6 h, the ISRE reporter activity was measured. G protein derivatives showed a weak ability (usually ~20%) to suppress the polyI:C-mediated ISRE reporter activity as

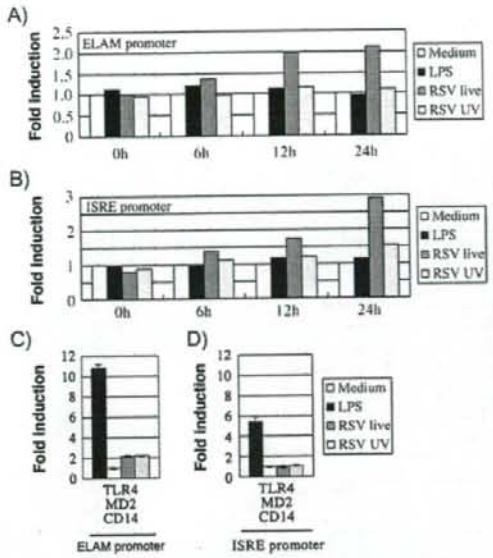

Fig. 3. Replication-dependent promoter activation by live RSV. (Panels A and B) Live but not UV-irradiated RSV activates the ELAM and ISRE promoter. HEK293 cells were transfected with pGV-E2/huELAM or pISRE-Luc and treated with the indicated stimulants as in Fig. 1(E). At timed intervals, luciferase reporter activity was determined for ELAM (A) and ISRE (B) activation. (Panels C and D) HEK293 cells with the ELAM or ISRE reporters were transfected with the plasmid set for TLR4 expression. Twenty-four hours later, cells were washed and treated with RSV (MOI = 0.5), LPS or medium. Six hours after incubation, reporter assay was performed as for ELAM (C) and ISRE (D). In either case, fold induction against medium is indicated. One of three similar experiments is shown.

compared with the vector transfectant (Fig. 6A). With the exception of the G protein, polyI:C-dependent ISRE activation was not affected by the expression of the RSV envelope proteins (Fig. 6A). The result was reproducible under the conditions where proteins were expressed to similar levels. Over-expressing RSV sG protein appears to externally inhibit the TLR3-mediated IFN-β-inducing event.

Since the sG protein maintained its inhibitory effect, we examined the ISRE inhibition by increasing doses of RSV sG protein using the TLR3 or TLR4 system. The culture supernatants from HEK293 cells transfected with the RSV sG (sGncFlag) plasmid were collected as a source of sG and used in the reporter assay. The supernatant of HEK293 cells with vector only was similarly prepared as a control. Cells were transfected with relevant plasmids for the TLR assay, and after 24 h, the cells were stimulated with LPS, polyI:C or media (presence or absence of the RSV sG protein for 6 h (Fig. 6B and C). ISRE activation by LPS–TLR4 (Fig. 6B) and polyI:C–TLR3 (Fig. 6C) were clearly inhibited by the exogenously added sG protein in a dose-dependent manner. These data suggest that it is the G protein that inhibits the TLR3/4-mediated IFN-β-inducing pathway.

Exogenously added RSV G protein suppresses IFN-β production in mDCs

It remained undetermined whether the extrinsic G protein physiologically controls mDC function. We determined IFN-β production in mDCs by stimulation with sG protein. The sG-mediated suppression of IFN production was endorsed with mDCs stimulated with polyI:C or LPS using ELISA (Fig. 7A). Finally, the purified F-protein-mediated IFN-β production was also blocked by RSV-G protein (Fig. 7B). Using the early-phase IFN-β mRNA determination assay by quantitative PCR (Fig. 2A), we checked whether exogenously added sG protein has an ability to inhibit RSV-mediated early (<2 h) induction of the IFN-β message in mDCs. The conditioned medium containing sG protein, if pre-incubated with mDCs, partially suppressed the increase of the IFN-β message by live and UV-irradiated RSV up to 4 h p.i. in mDCs (data not shown). Hence, additional sG protein can modulate mDC functions including IFN-β induction raised secondary to RSV–mDC interaction.

The sG protein selectively inhibits TICAM-1/TRIF signaling

Recent reports described the presence of TLR-independent dsRNA-mediated type I IFN-inducing pathways (38). RIG-I and MDA5 are the sensors responsible for virus RNA recognition (39). These molecules reside in the cytoplasm where they recognize dsRNA or viral RNA-specific patterns and activate IKKε and TBK1 through the adaptor MAVS (IPS-1) (18). To examine whether the sG protein could inhibit the cytoplasmic pathway, we transfected HEK293 cells with reporter plasmids together with the plasmids for the constitutively active form of RIG-I or MDA5 (ΔRIG-I or MDA5N), IPS-1, TICAM-1, IKKε or TBK-1. The IFN-inhibitory effect of the sG protein, UV-irradiated RSV and UV-irradiated MV (as a control) was assessed using the reporter assay after 6 h. The sG protein and UV-irradiated RSV inhibited ISRE activity by TICAM-1, but not by other cytoplasmic factors including RIG-I and MAVS (Fig. 8A). The TICAM-1-mediated ISRE activation was inhibited in a sG dose-dependent manner (Fig. 8B). UV-irradiated MV did not inhibit ISRE activation in terms of all the transfected constructs (Fig. 8A). IKKε/TBK-1-mediated ISRE response was not affected by the sG protein added and rather increased by stimulation with UV-irradiated RSV (data not shown), although the latter reason as yet unknown. Hence, we can conclude that the sG protein selectively inhibits the TICAM-1-signaling pathway upstream of the IRF-3 kinases, but not the RIG-I/MDA5 pathway. This issue was confirmed using TICAM-1- and MAVS-silencing HeLa cells made by the RNAi technology (M. Matsumoto and T. Seya, unpublished data).

Discussion

We demonstrated that mDCs produce only minute amounts of IFN-β in response to live and UV-irradiated RSV while mDCs induce TNF-α to mature in response to the same RSV treatment. IFN-β is poorly produced only when whole-virus particles exogenously attack for mDC infection. This situation may coincide with RSV-mediated mDC maturation which is also triggered by RSV attachment to the host cell surface.